

AD-A089 443

NAVAL OCEAN SYSTEMS CENTER SAN DIEGO CA
IMPLEMENTATION AND EVALUATION OF THE DISTURBANCE AMPLIFICATION --ETC(U)
MAR 80 T S MAUTNER
NOSC/TD-340

F/G 20/4

UNCLASSIFIED

NL

1 OF 1
AD A
10-24-03

NOSC

END
DATE
FILMED
10-80
DTIC

56
LEVEL #

12

NOSC

NOSC TD 340

AD A089443

NOSC TD 340

Technical Document 340

IMPLEMENTATION AND EVALUATION
OF THE DISTURBANCE AMPLIFICATION
IN BOUNDARY LAYERS (DABL)
COMPUTER PROGRAM:
A USER'S MANUAL

T. S. Mautner

March 1980

Prepared for
Naval Sea Systems Command

41N-1/TI-111

Approved for public release; distribution unlimited

NAVAL OCEAN SYSTEMS CENTER
SAN DIEGO, CALIFORNIA 92152

DTIC
ELECTE
SEP 24 1980

A

80 9 24 019

DDC FILE COPY



NAVAL OCEAN SYSTEMS CENTER, SAN DIEGO, CA 92152

A N A C T I V I T Y O F T H E N A V A L M A T E R I A L C O M M A N D

SL GUILLE, CAPT, USN
Commander

HL BLOOD
Technical Director

ADMINISTRATIVE INFORMATION

The work reported herein was performed as a portion of the research conducted at NOSC within the Torpedo Hydrodynamics and Hydroacoustics Program funded by the Naval Sea Systems Command (NAVSEA 63R31), Dr. T. E. Peirce, Program Manager. The work was performed in the Fluid Mechanics Branch (Code 6342), Hydromechanics Division of the Fleet Engineering Department.

Released by
J. H. Green, Head
Hydromechanics Division

Under authority of
R. H. Hearn, Head
Fleet Engineering Department

UNCLASSIFIED

SECURITY CLASSIFICATION OF THIS PAGE (When Data Entered)

REPORT DOCUMENTATION PAGE		READ INSTRUCTIONS BEFORE COMPLETING FORM
1. REPORT NUMBER TD 340	2. GOVT ACCESSION NO. AD-A089443	3. RECIPIENT'S CATALOG NUMBER
4. TITLE (and Subtitle) IMPLEMENTATION AND EVALUATION OF THE DISTURBANCE AMPLIFICATION IN BOUNDARY LAYERS (DABL) COMPUTER PROGRAM: A USER'S MANUAL		5. TYPE OF REPORT & PERIOD COVERED Research
		6. PERFORMING ORG. REPORT NUMBER
7. AUTHOR(s) T. S. Mautner		8. CONTRACT OR GRANT NUMBER(s)
9. PERFORMING ORGANIZATION NAME AND ADDRESS Naval Ocean Systems Center San Diego, CA 92152		10. PROGRAM ELEMENT, PROJECT, TASK AREA & WORK UNIT NUMBERS
11. CONTROLLING OFFICE NAME AND ADDRESS		12. REPORT DATE March 1980
		13. NUMBER OF PAGES 50
14. MONITORING AGENCY NAME & ADDRESS (if different from Controlling Office)		15. SECURITY CLASS. (of this report) Unclassified
		15a. DECLASSIFICATION/DOWNGRADING SCHEDULE
16. DISTRIBUTION STATEMENT (of this Report) Approved for public release; distribution unlimited		
17. DISTRIBUTION STATEMENT (of the abstract entered in Block 20, if different from Report)		
18. SUPPLEMENTARY NOTES		
19. KEY WORDS (Continue on reverse side if necessary and identify by block number) DABL TAPS Disturbance amplification		
20. ABSTRACT (Continue on reverse side if necessary and identify by block number) This report describes the implementation and evaluation of the Fortran IV computer program DABL (Disturbance Amplification in Boundary Layers) which calculates the growth of small disturbances in laminar boundary layers.		

DD FORM 1 JAN 73 1473

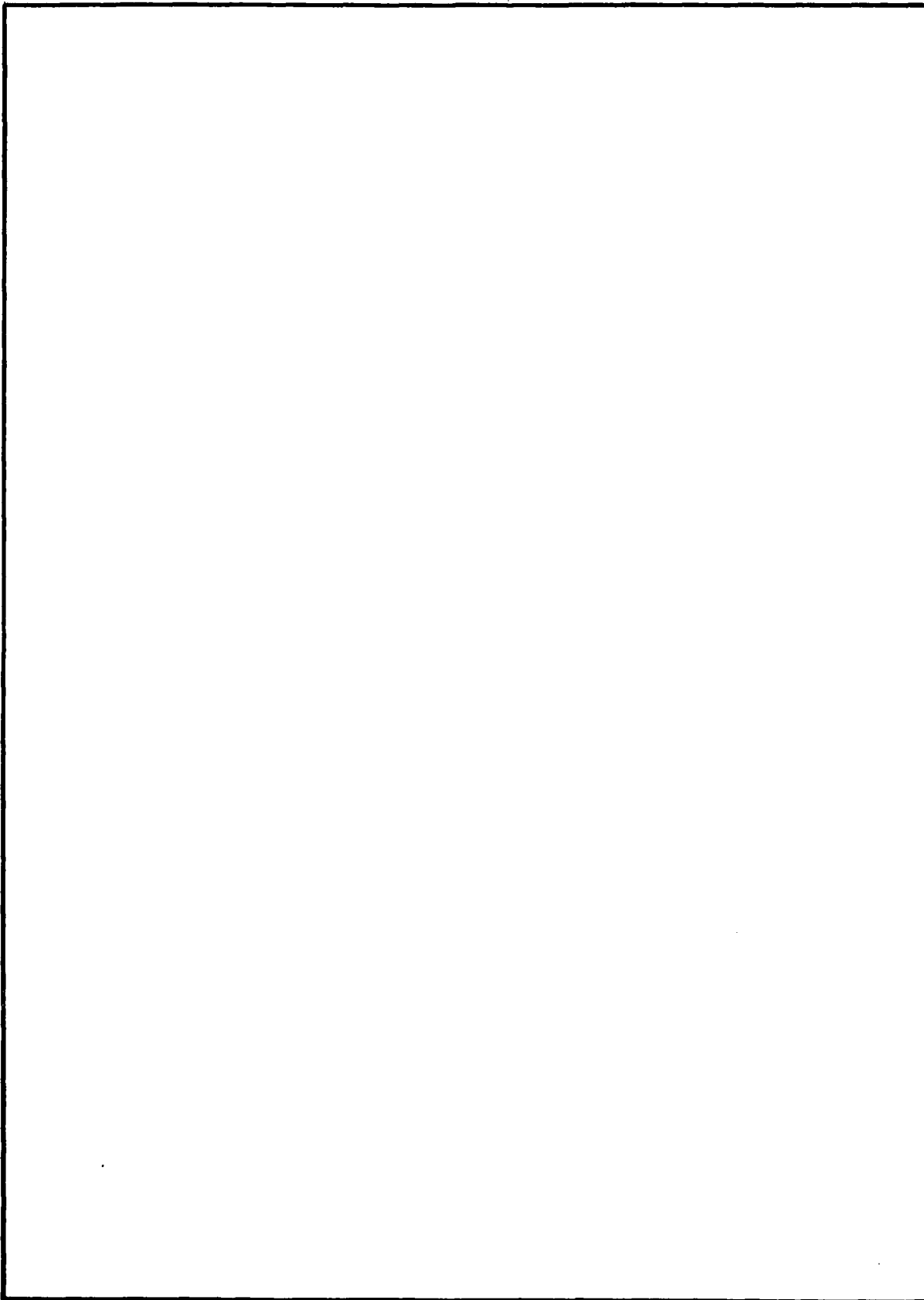
- EDITION OF 1 NOV 65 IS OBSOLETE
S/N 0102-LF-014-6601

UNCLASSIFIED

SECURITY CLASSIFICATION OF THIS PAGE (When Data Entered)

UNCLASSIFIED

SECURITY CLASSIFICATION OF THIS PAGE (When Data Entered)



UNCLASSIFIED

SECURITY CLASSIFICATION OF THIS PAGE (When Data Entered)

CONTENTS

DEFINITION OF TERMS . . .	page 3
INTRODUCTION . . .	5
TWO-DIMENSIONAL GEOMETRY . . .	6
AXISYMMETRIC GEOMETRY . . .	12
COMPUTER PROGRAM USAGE . . .	23
Definition of the Input Variables . . .	23
Method of Inputting Data Tables . . .	25
Program Input Scheme . . .	26
COMPUTER PRINTOUT . . .	29
Included Items . . .	29
Printout Definitions . . .	29
SUMMARY . . .	32
REFERENCES . . .	33
APPENDIX A: Computer Listing - Heated Flat Plate . . .	34
APPENDIX B: Computer Listing - Heated 9:1 Ellipsoid . . .	42

Accession For	
NTIS CSMAJ	<input checked="checked" type="checkbox"/>
DDP 148	<input type="checkbox"/>
Unprocessed	<input type="checkbox"/>
Justification	<input type="checkbox"/>
By	
Distribution	
Available to	
Dist.	available or special
A	

ILLUSTRATIONS

1. Comparison of the neutral stability curves of a flat plate . . . page 7
2. Comparison of the disturbance amplification ratios of a flat plate . . . 9
3. Comparison of the neutral stability points of a flat plate with 2.78°C surface overheat . . . 11
4. Potential flow velocity distribution of a 9:1 ellipsoid . . . 13
5. Skin friction coefficient of a 9:1 ellipsoid - $R_L \cong 4.5 \times 10^6/\text{ft}$. . . 13
6. Boundary layer shape factor of a 9:1 ellipsoid - $R_L \cong 4.5 \times 10^6/\text{ft}$. . . 14
7. Displacement thickness Reynolds number of a 9:1 ellipsoid - $R_L \cong 4.5 \times 10^6/\text{ft}$. . . 14
8. Computed growth rates of a 9:1 ellipsoid for $\omega_f = 0.486 \times 10^{-4}$ - $R_L \cong 4.5 \times 10^6/\text{ft}$. . . 15
9. Computed growth rates of a 9:1 ellipsoid for $\omega_f = 0.32 \times 10^{-4}$ - $R_L \cong 4.5 \times 10^6/\text{ft}$. . . 16
10. Comparison of the computed amplification ratios of a 9:1 ellipsoid for $\omega_f = 0.486 \times 10^{-4}$ and $\omega_f = 0.32 \times 10^{-4}$ - $R_L \cong 4.5 \times 10^6/\text{ft}$. . . 17
11. Surface temperature distribution of a 9:1 ellipsoid - $R_L \cong 4.49 \times 10^6/\text{ft}$. . . 18
12. Skin friction coefficient of a heated 9:1 ellipsoid - $R_L \cong 4.49 \times 10^6/\text{ft}$. . . 18
13. Boundary layer shape factor of a heated 9:1 ellipsoid - $R_L \cong 4.49 \times 10^6/\text{ft}$. . . 18
14. Displacement thickness Reynolds number of a heated 9:1 ellipsoid - $R_L \cong 4.49 \times 10^6/\text{ft}$. . . 19
15. Computed growth rates of a heated 9:1 ellipsoid for $\omega_f = 0.32 \times 10^{-4}$ - $R_L \cong 4.49 \times 10^6/\text{ft}$. . . 20
16. Computed growth rates of a heated 9:1 ellipsoid for $\omega_f = 0.18 \times 10^{-4}$ - $R_L \cong 4.49 \times 10^6/\text{ft}$. . . 21
17. Comparison of the computed amplification ratios of a heated 9:1 ellipsoid - $R_L \cong 4.49 \times 10^6/\text{ft}$. . . 22
18. Input direction for the axisymmetric body coordinates . . . 27
19. Input direction for the two-dimensional body coordinates . . . 28

TABLES

1. Summary of the computed values for the neutral curve of an unheated flat plate . . . 8
2. Summary of the computed values for the neutral curve of a heated flat plate ($\Delta T = 2.78^{\circ}\text{C}$) . . . 10

DEFINITION OF TERMS

A/A_0	Disturbance Amplification Ratio
C_f	Skin Friction Coefficient
e^N	The Amplification Ratio ($= A/A_0$) according to linear stability theory
f	Disturbance Frequency – Hz
H	Boundary Layer Shape Factor
L	Reference Length
R_L	Reynolds Number $= U_\infty L/\nu_\infty$
R_δ^*	Displacement Thickness Reynolds Number $= U_\infty \delta^*/\nu_\infty$
T	Temperature
U_∞	Free Stream Velocity
$-\alpha_i^*$	Local Relative Growth Rate of a Disturbance
δ^*	Displacement Thickness
ν_∞	Free Stream Kinematic Viscosity
ω_f	Nondimensional Disturbance Frequency $= 2\pi f \nu_\infty / U_\infty^2$

INTRODUCTION

This report describes the implementation and evaluation of the Fortran IV computer program DABL (Disturbance Amplification in Boundary Layers — developed at the David Taylor Naval Ship Research and Development Center (DTNSRDC) by vonKerczek and Groves, 1978) which calculates the growth of small disturbances in laminar boundary layers. DABL calculates the amplification ratios, A/A_0 , for heated or unheated, two-dimensional or axisymmetric, incompressible laminar boundary layers. The boundary layer is assumed to be steady and has constant density with the fluid viscosity varying with temperature. The DABL code requires only the body coordinates, surface temperature distribution and body Reynolds number to compute the spatial amplification ratios as a function of arc length and nondimensional disturbance frequency using parallel, viscous flow, linear stability theory. The resulting amplification ratio distribution can be used to locate boundary layer transition via the e^N method.

This report makes no attempt to discuss or evaluate the theoretical and numerical methods used by DABL in computing the boundary layer properties and in performing the boundary layer stability analysis. vonKerczek and Groves (1978) discussed these topics in detail. However, this report does present several examples used to evaluate DABL as modified by the author and adapted to the NOSC UNIVAC 1110 Computer.

Upon receipt of the DABL Program from DTNSRDC, the computer code was altered (to be compatible with UNIVAC 1110) and compiled in ASCII Fortran utilizing a segmented execution mode to conform to the 65K storage limit of the NOSC system. Prior to any further changes, DABL was checked for proper execution using the examples of vonKerczek and Groves (1978).

After the DABL code was operating properly, the following additions/changes were incorporated into the code:

1. The program output was expanded to include both the original and normalized body coordinates and, in the case of heated bodies, the surface temperature distribution.
2. The option to read and write the boundary layer data to mass storage was added.
3. The fluid property definitions were expanded to include air, as well as water, boundary layers.
4. Options were included to allow the stability calculations to proceed regardless of the calculated amplification ratio value and to begin the stability automatic start routine at a prescribed body location.
5. The step function surface temperature distribution was changed to allow the distribution to end prior to the end of the body.

The remainder of the report is divided into several sections. First, DABL was used to compute the neutral stability points for an unheated and heated flat plate and the amplification ratios at several disturbance frequencies for the unheated plate. These results are compared with theory and experiment. Next, a comparison is made between the values of skin friction, shape factor, growth rates and amplification ratios computed by DABL and TAPS (Transition Analysis Program System) for both a heated and unheated 9:1 ellipsoid. Thirdly, a complete description of the input/output variables and program input scheme of DABL is presented. Finally, abbreviated listings of the computer output for the heated flat plate and the heated 9:1 ellipsoid are included as examples.

Although many of the descriptions found in the original DABL report (vonKerczek and Groves, 1978) are repeated here, the input format for the NOSC version of DABL has been changed completely. Anyone desiring to use this program should contact the author and a listing, card deck or tape and check solutions will be provided.

TWO-DIMENSIONAL GEOMETRY

To evaluate the two-dimensional option of the DABL code, a flat plate geometry was chosen. The test plate is 0.25 inches thick and has a sharp leading edge with a 1.8 degree half angle. There is good agreement with the potential flow velocities computed by DABL and the Douglas Two-Dimensional Cascade Potential Flow Program (Giesing, 1964). The plate has a nearly zero pressure gradient at a zero angle of attack. Overall plate lengths of one and 12 feet were used in the analysis. The coordinates of the one-foot plate and the potential flow velocities are given in Appendix A.

The neutral stability curves for both an unheated plate and a heated plate with a constant surface overheat of 2.78°C were calculated using the automatic starting option of DABL. For each plate length and Reynolds number, R_L/ft , the neutral stability points (where $-\alpha^* = 0$) were located and the corresponding displacement thickness Reynolds number and nondimensional frequency were tabulated and plotted.

Figure 1 compares the neutral stability points computed by DABL (also found in Table 1) with the experimental results of Schubauer and Skramstad (1948) and the theoretical results presented by Ross et al (1970). As the R_L/ft was increased, DABL's automatic starting method calculated nondimensional frequencies ω_f which resulted in neutral points falling within the neutral curve of Ross et al. However, if for a particular R_L/ft , the starting ω_f is decreased, the DABL calculated neutral points fall closer to theoretical and experimental values.

In Figure 2, a comparison is made between the amplification ratios A/A_0 computed by DABL and the theoretical curves of Jordinson (1970) and the experimental data presented by Ross et al (1970). Agreement is good within the common regions of comparison. The additional amplification ratios for $R_L/\text{ft} = 2.0 \times 10^6$ and 5.0×10^6 have been included as further demonstration of DABL's results; however, no comparisons are made.

Finally, the neutral stability points for a heated plate (constant $\Delta T = 2.78^{\circ}\text{C}$) were calculated using DABL (also found in Table 2) and are compared to the experimental results of Strazisar (1976) in Figure 3. As in the unheated case, DABL's automatic starting mode computes frequencies ω_f which result in neutral points falling within the neutral zone defined by Strazisar. In general, DABL produces conservative estimates for the onset of disturbance amplification.

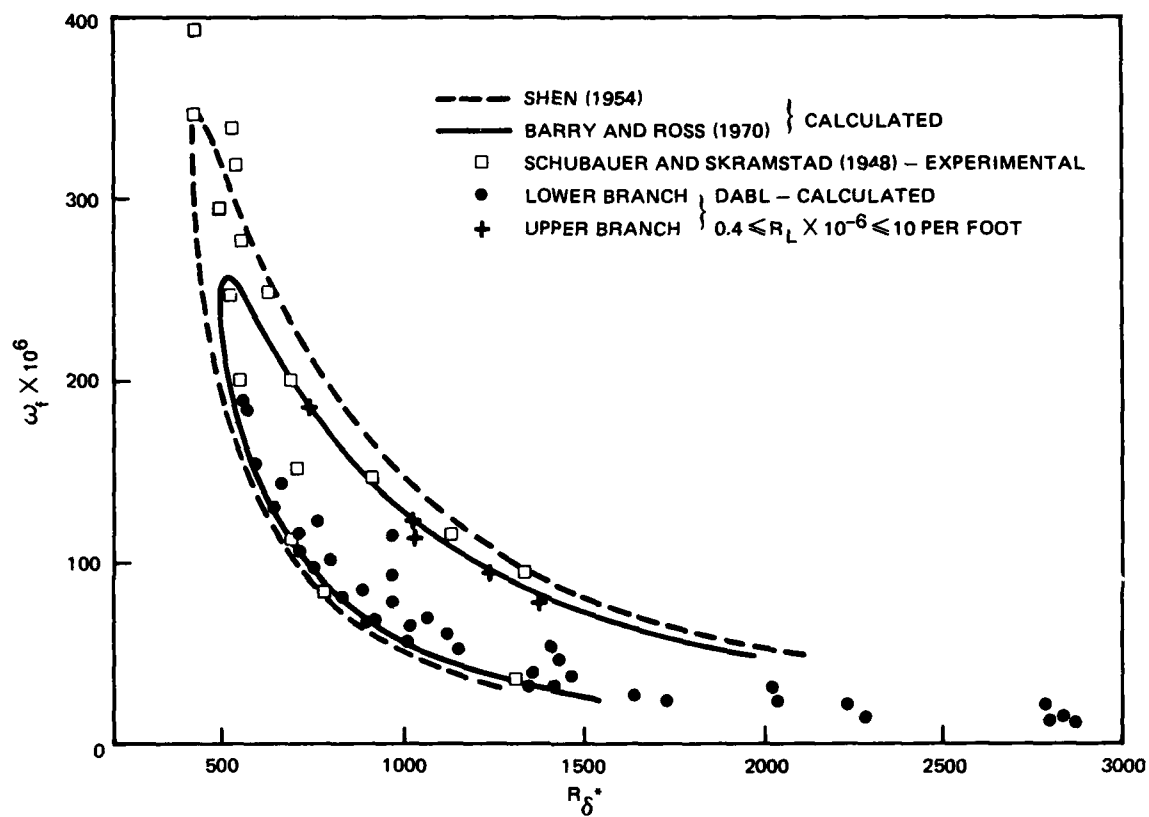


Figure 1. Comparison of the neutral stability curves of a flat plate.

Plate Length, ft	$R_L \times 10^{-6}/\text{ft}$	$\omega_f \times 10^6$	R_δ^*		Fluid
1.00	0.40	189.56	558	730	Water
		157.34	596		
		130.59	645		
		108.39	704		
	0.50	185.54	570	740	
		154.00	605		
		127.82	655		
		106.09	712		
		88.06	782		
	1.00	143.57	662		
		119.16	700		
		98.90	753		
		82.09	824		
		68.13	902		
	2.00	122.42	755	1045	
		101.60	794		
		84.33	880		
		70.00	935		
		58.10	1005		
	5.00	113.96	970	1030	
		94.59	962	1245	
		78.51	970	1385	
		65.16	1015		
		54.08	1150		
	10.00	41.00	1360		
		34.00	1420		
		28.00	1640		
		23.50	1730		
12.0	2.00	56.54	1410		
		46.93	1430		
		38.95	1465		
	5.00	30.87	2015		
		25.63	2045		
		21.27	2215		
		17.65	2285		
	10.00	21.36	2780		
		20.09	2770	4025	
		17.73	2800		
		16.68	2820	4220	
		13.84	2870	5085	

Table 1. Summary of the computed values for the neutral curve of an unheated flat plate.

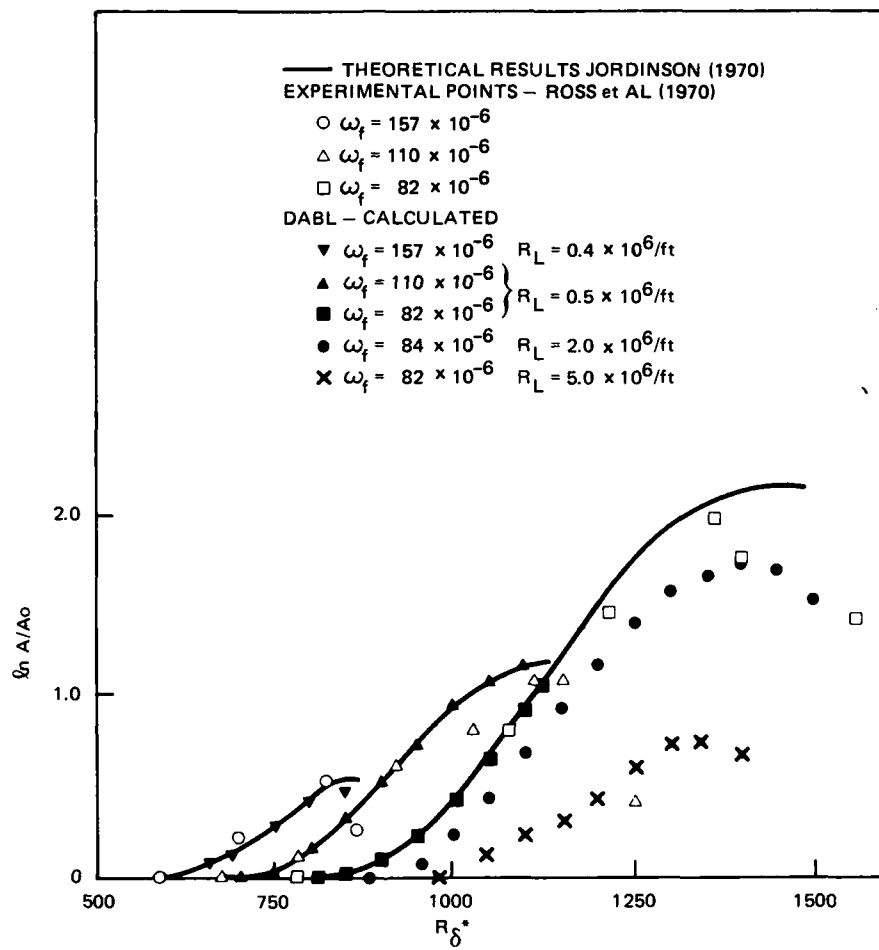


Figure 2. Comparison of the disturbance amplification ratios of a flat plate.

Plate Length, ft	$R_L \times 10^{-6}/\text{ft}$	$\omega_f \times 10^6$	R_δ^*		Fluid	
1.00	0.25	173.43	595	900	Water	
	0.50	163.72	615			
		135.89	655			
	1.00	139.30	675			
		115.62	724			
		95.96	780			
		79.65	845			
		66.11	930			
	2.00	118.62	762			785
		118.62	855			1020
		98.46	864			1195
		81.72	890			
		67.83	948			
		56.30	1028			
	5.00	93.70	945			1042
		93.70	1137			1208
		77.77	965			1310
		64.55	1100			1642
		53.57	1137			
	5.00	114.85	800	830	Air	
		114.85	980	1040		
		95.33	960	1245		
		79.12	980			
		65.67	1022			
		54.51	1026			

Table 2. Summary of the computed values for the neutral curve of a heated flat plate ($\Delta T = 2.78^\circ\text{C}$).

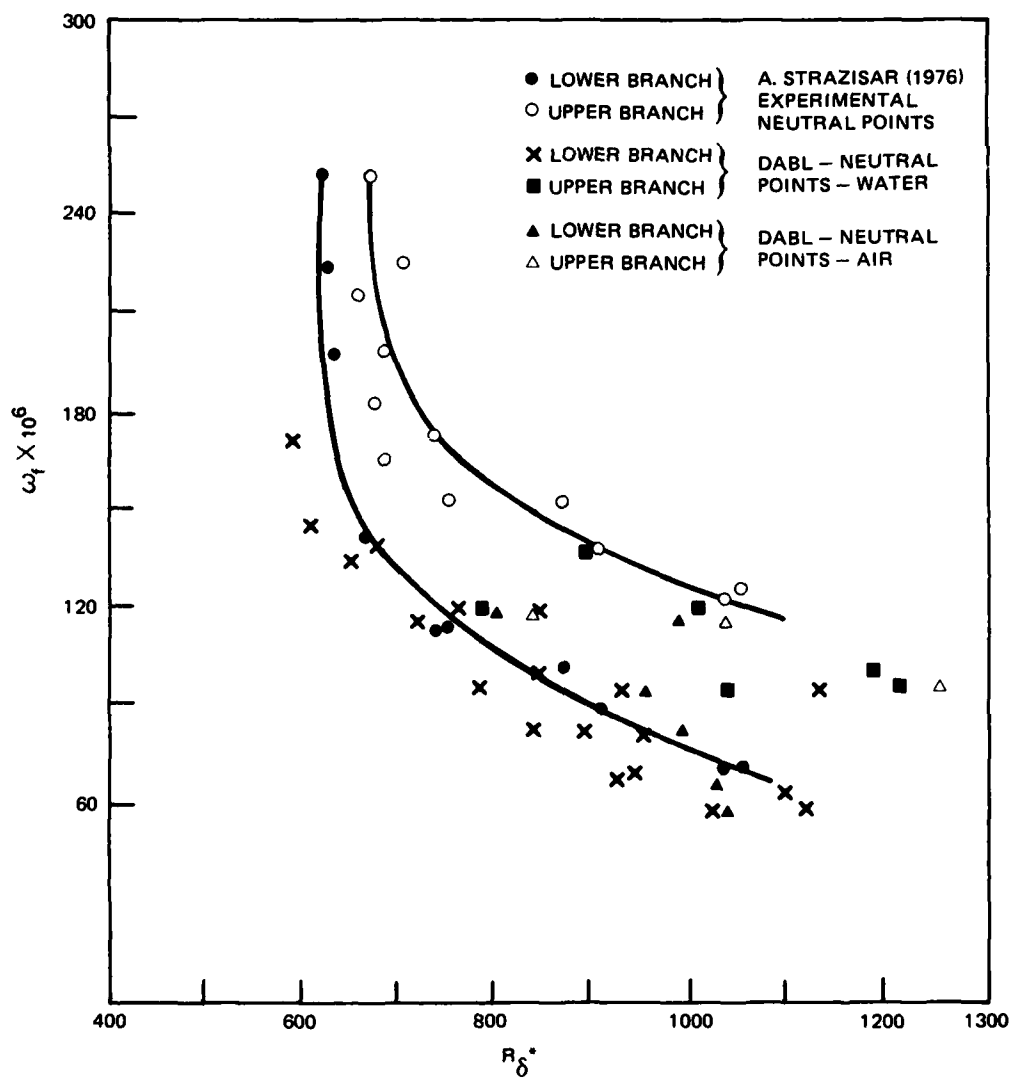


Figure 3. Comparison of the neutral stability points of a flat plate with 2.78°C surface overheat.

AXISYMMETRIC GEOMETRY

A 9:1 ellipsoid was selected to provide a comparison between the results of DABL and TAPS for both a heated and unheated axisymmetric body. The coordinates, potential flow velocities and surface temperature distribution of the ellipsoid are given in Appendix B while a comparison of the potential flow velocities computed by DABL and TAPS is shown in Figure 4.

First, for the unheated case, Figures 5, 6 and 7 compare the skin friction coefficient, boundary layer shape factor and displacement thickness Reynolds number as a function of arc length computed by DABL and TAPS at $R_L \cong 4.5 \times 10^6/\text{ft}$. In all cases there is good agreement between DABL and TAPS with slight differences occurring near the ellipsoid nose. Figures 8 and 9 compare the computed values of the disturbance growth rates for nondimensional frequencies $\omega_f = 0.32 \times 10^{-4}$ and $\omega_f = 0.486 \times 10^{-4}$, respectively. The corresponding amplification ratios are shown in Figure 10. Both the growth rates and amplification ratios of DABL and TAPS are in close agreement. It should be noted that the higher amplification ratios calculated by DABL are consistent with the results given by vonKerczek and Groves (1978).

For the heated case, the surface temperature distribution shown in Figure 11 was used by both DABL and TAPS for the ellipsoid at $R_L \cong 4.49 \times 10^6/\text{ft}$. Figures 12, 13 and 14 compare the skin friction coefficient, shape factor and displacement thickness Reynolds number computed by DABL and TAPS. The computed disturbance growth rates and amplification ratios for frequencies $\omega_f = 0.32 \times 10^{-4}$ and $\omega_f = 0.18 \times 10^{-4}$ are shown in Figures 15, 16 and 17. In all cases DABL produces larger growth rates and amplification ratios than TAPS. As stated by vonKerczek and Groves, linear stability theory is sensitive to the boundary layer shape factor and Figure 13 shows that DABL yields a slightly larger shape factor than TAPS which could account for the larger growth rates and amplification ratios. Figure 17 also compares the amplification ratios at $\omega_f = 0.22 \times 10^{-4}$ between DABL and TAPS and DABL's amplification ratios for a constant surface temperature difference, $\Delta T = 6.0\text{C}$. It can be concluded that DABL produces more conservative results as compared to TAPS.

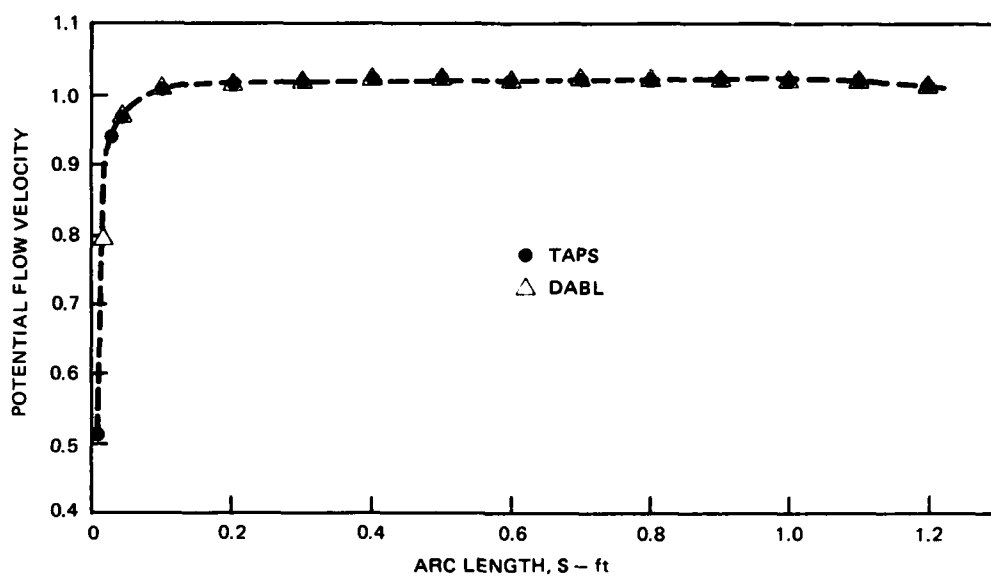


Figure 4. Potential flow velocity distribution of a 9:1 ellipsoid.

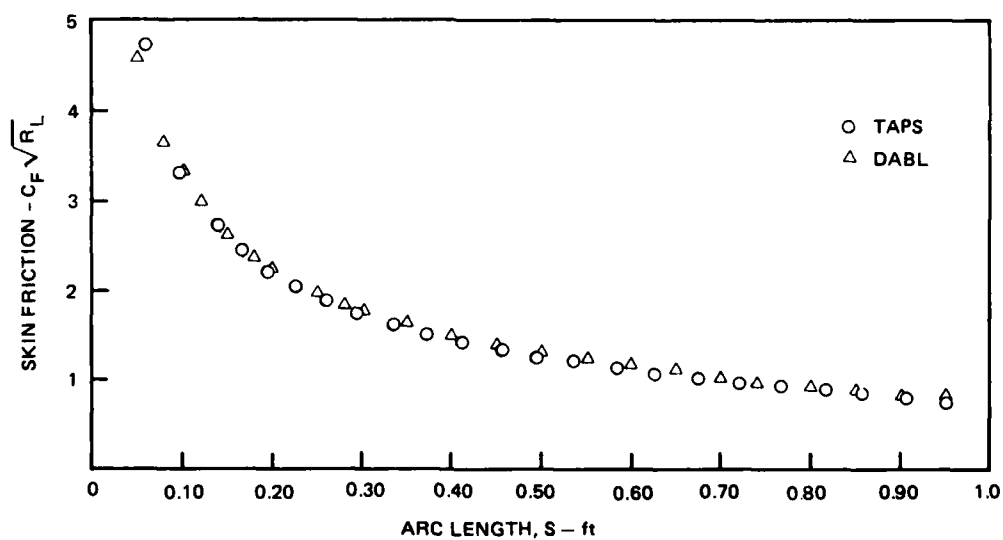


Figure 5. Skin friction coefficient of a 9:1 ellipsoid - $R_L = 4.5345455 \times 10^6/\text{ft}$.

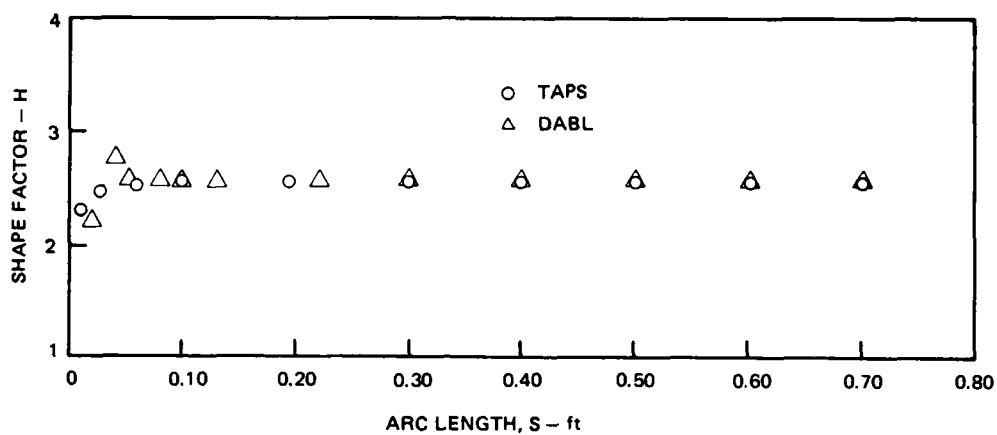


Figure 6. Boundary layer shape factor of a 9:1 ellipsoid - $R_L = 4.5345455 \times 10^6/\text{ft}$

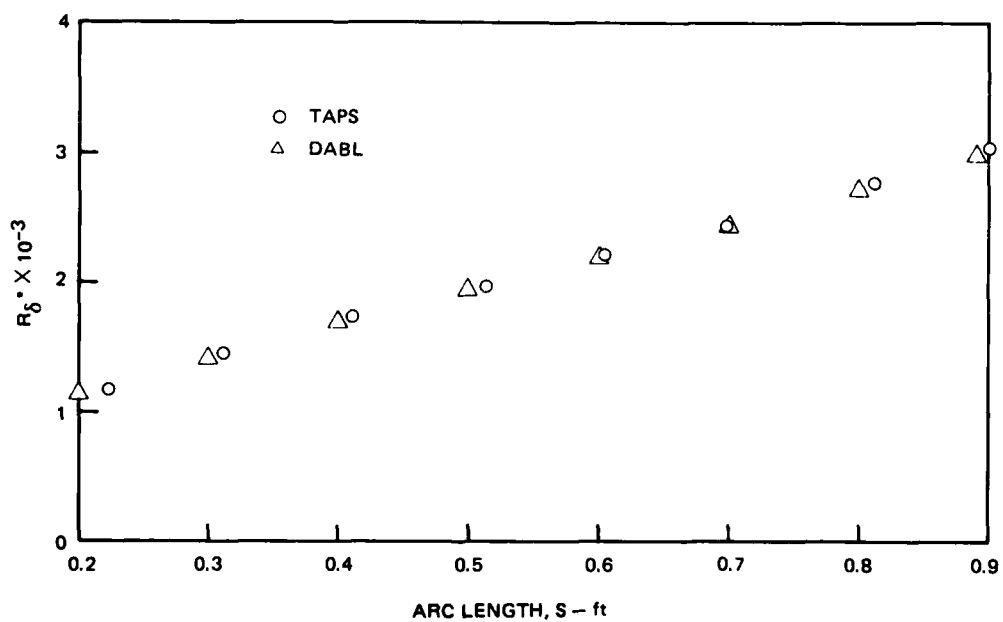


Figure 7. Displacement thickness Reynolds number of a 9:1 ellipsoid - $R_L = 4.5345455 \times 10^6/\text{ft}$.

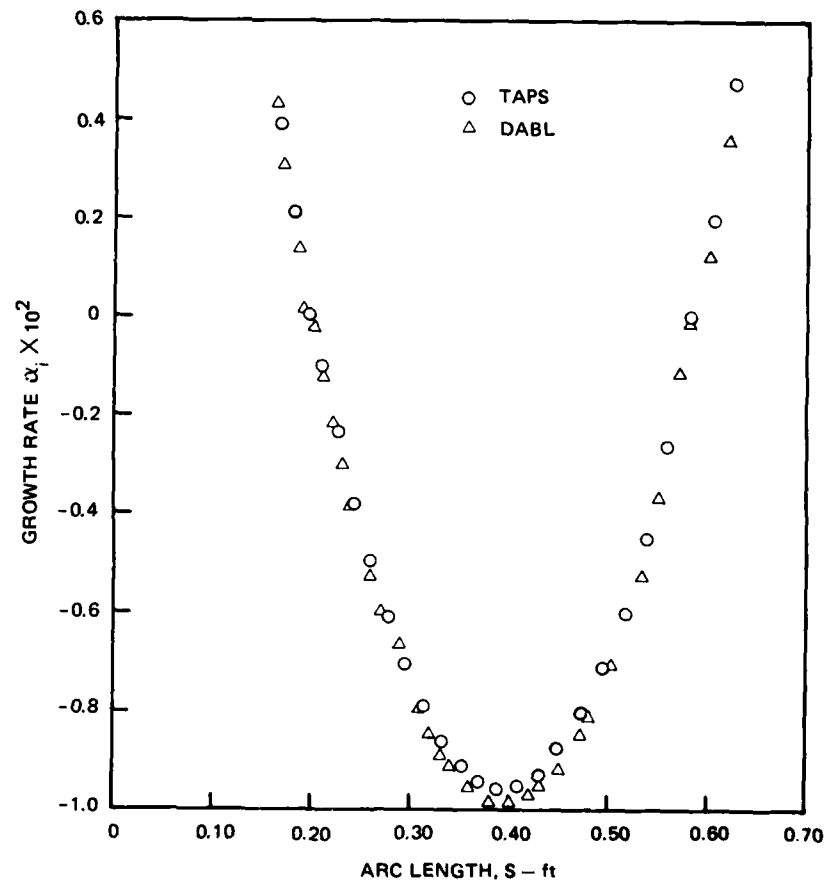


Figure 8. Computed growth rates of a 9:1 ellipsoid for $\omega_f = 0.486 \times 10^{-4}$ - $R_L = 4.5345455 \times 10^6/\text{ft}$.

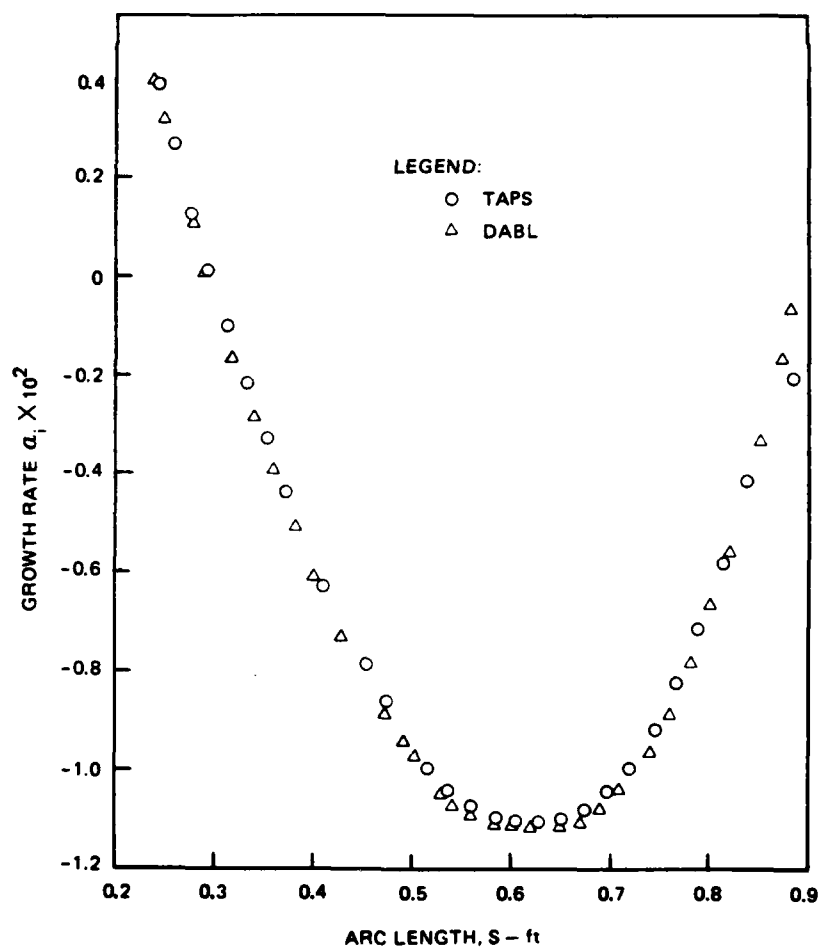


Figure 9. Computed growth rates of a 9:1 ellipsoid for $\omega_f = 0.32 \times 10^{-4}$ - $R_L = 4.5345455 \times 10^6/\text{ft}$.

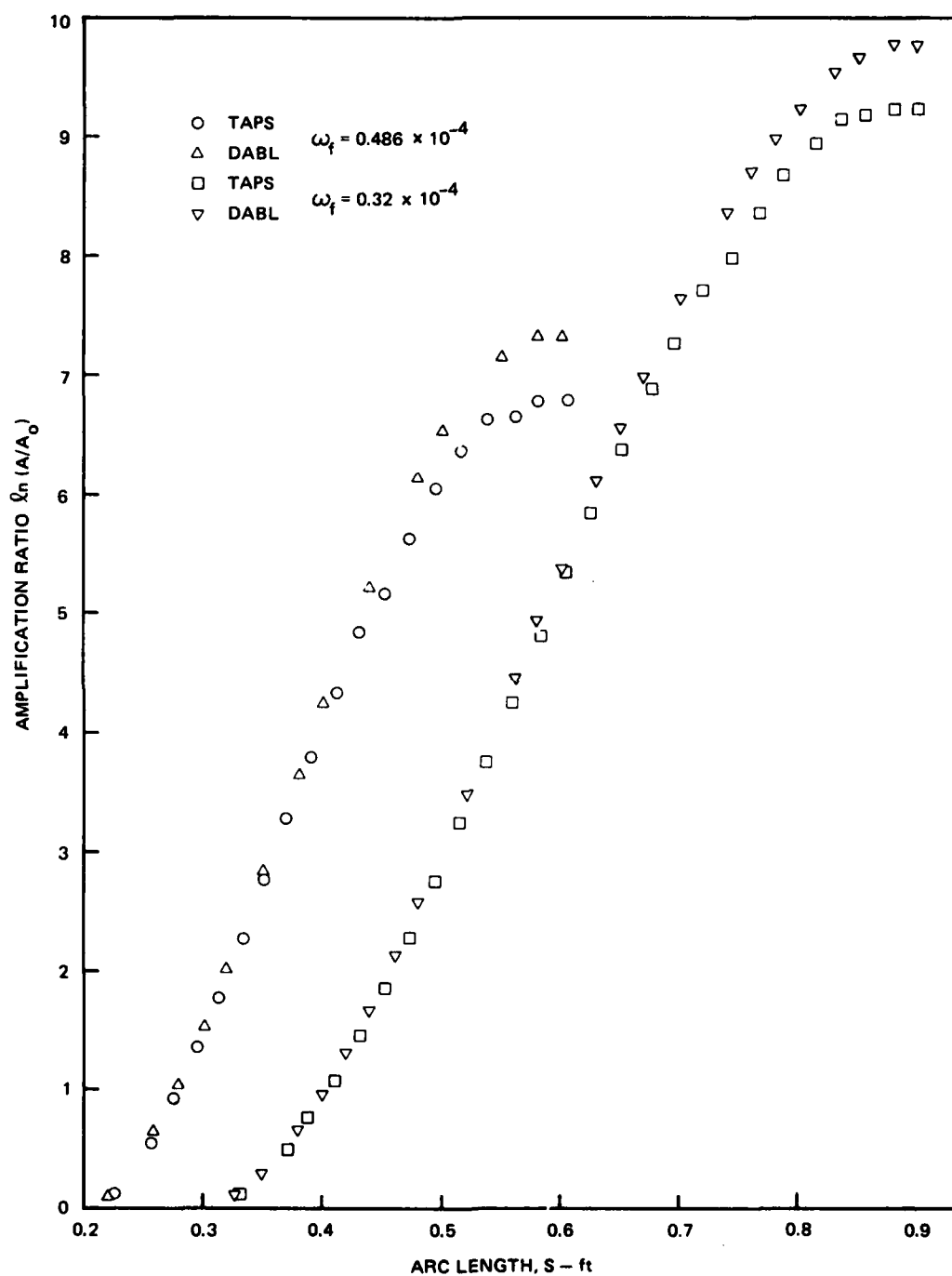


Figure 10. Comparison of the computed amplification ratios of a 9:1 ellipsoid for $\omega_f = 0.486 \times 10^{-4}$ and $\omega_f = 0.32 \times 10^{-4}$ - $R_L = 4.5345455 \times 10^6/\text{ft}$.

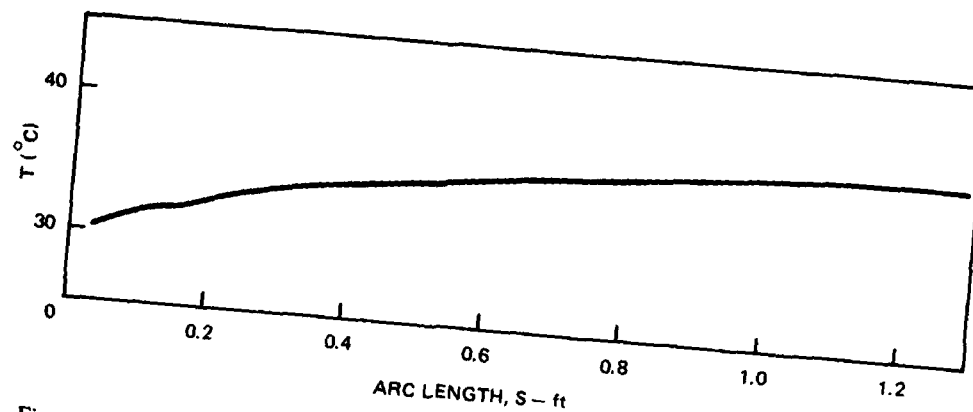


Figure 11. Surface temperature distribution of a 9:1 ellipsoid - $R_L = 4.4901734 \times 10^6/\text{ft}$.

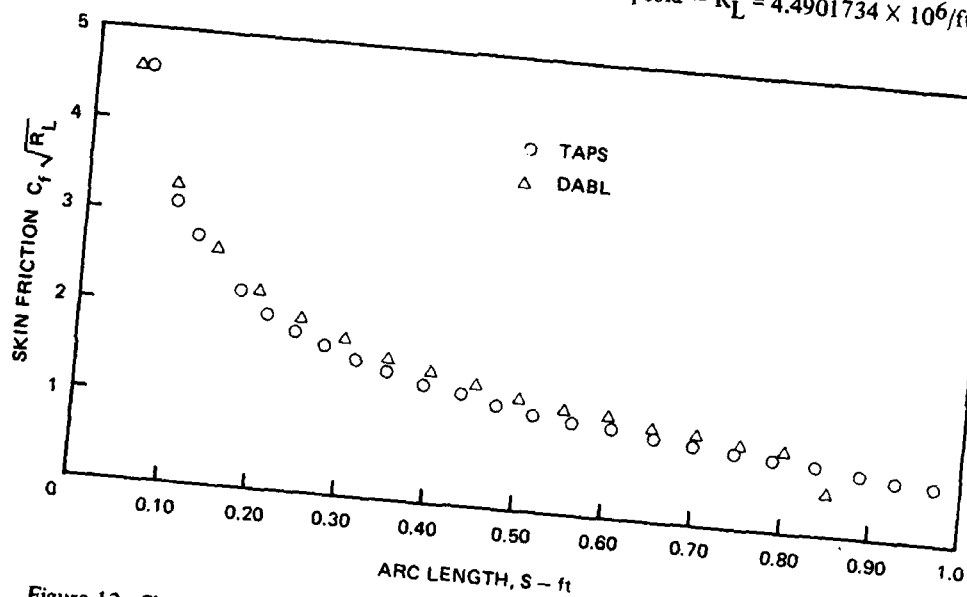


Figure 12. Skin friction coefficient of a heated 9:1 ellipsoid - $R_L = 4.4901734 \times 10^6/\text{ft}$.

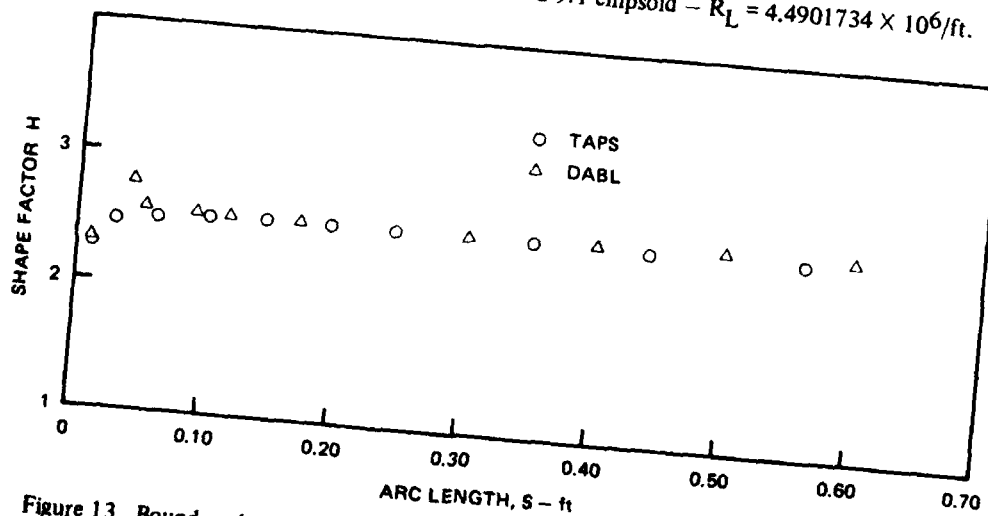


Figure 13. Boundary layer shape factor of a heated 9:1 ellipsoid - $R_L = 4.4901734 \times 10^6/\text{ft}$.

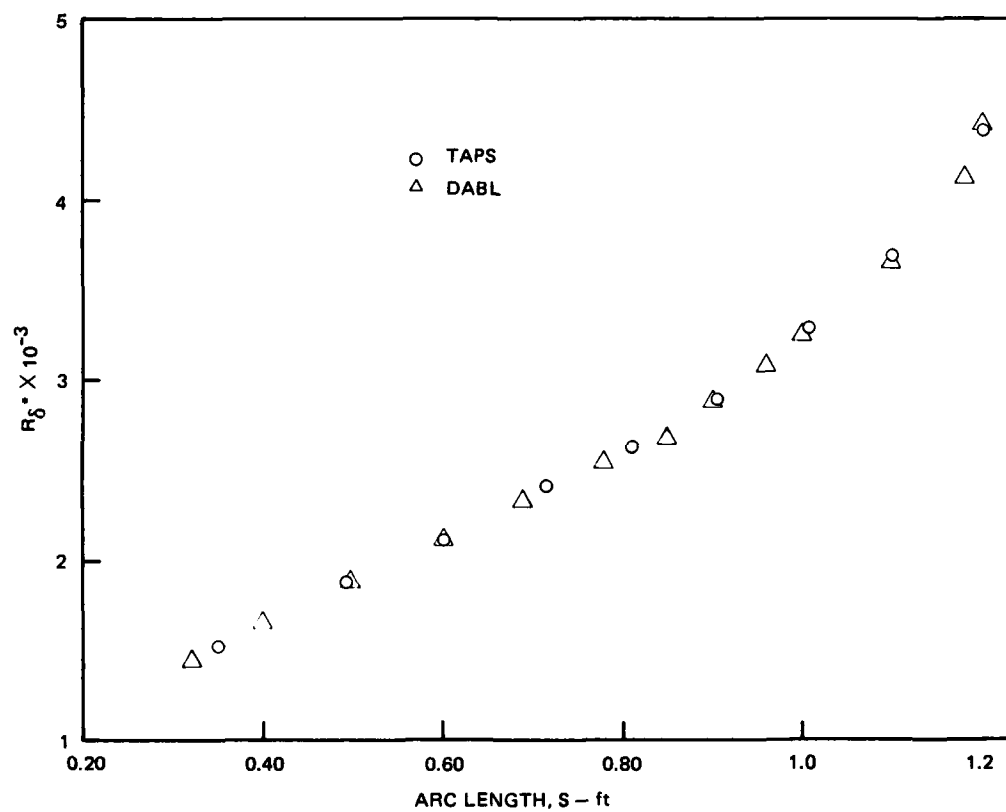


Figure 14. Displacement thickness Reynolds number of a heated 9:1 ellipsoid –
 $R_L = 4.4901734 \times 10^6/\text{ft}$.

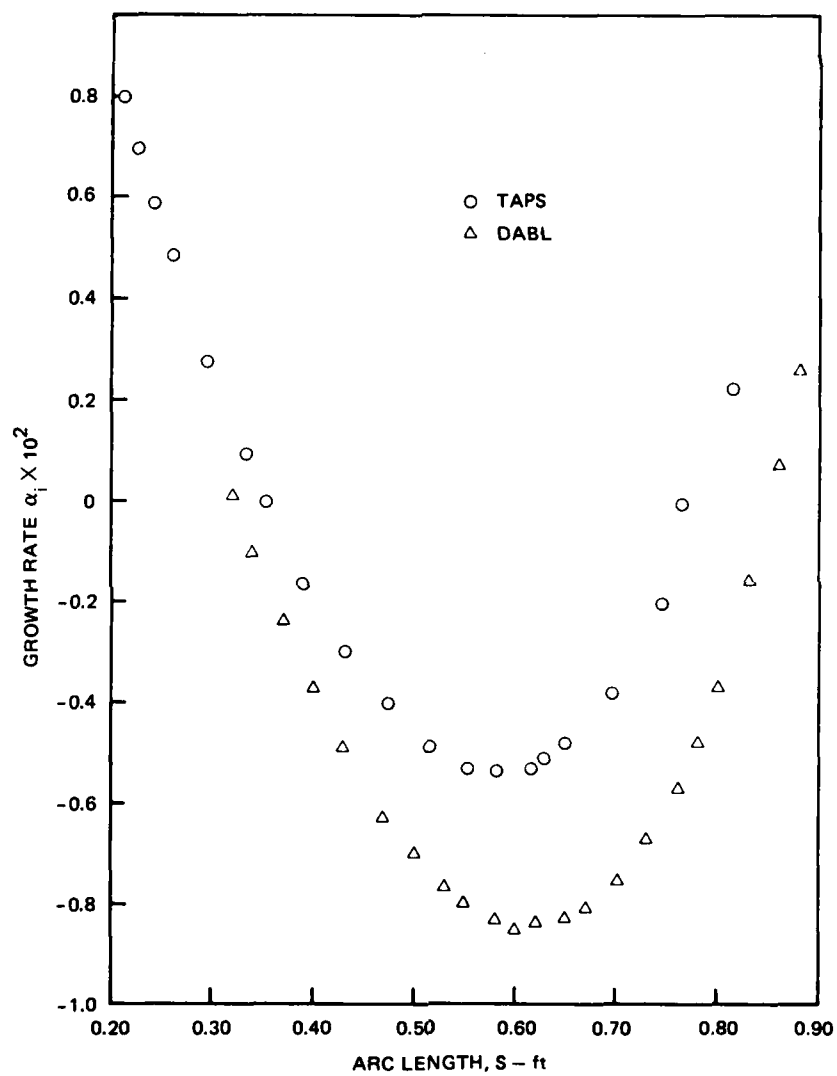


Figure 15. Computed growth rates of a heated 9:1 ellipsoid for $\omega_f = 0.32 \times 10^{-4}$ - $R_L = 4.4901134 \times 10^6/\text{ft}$.

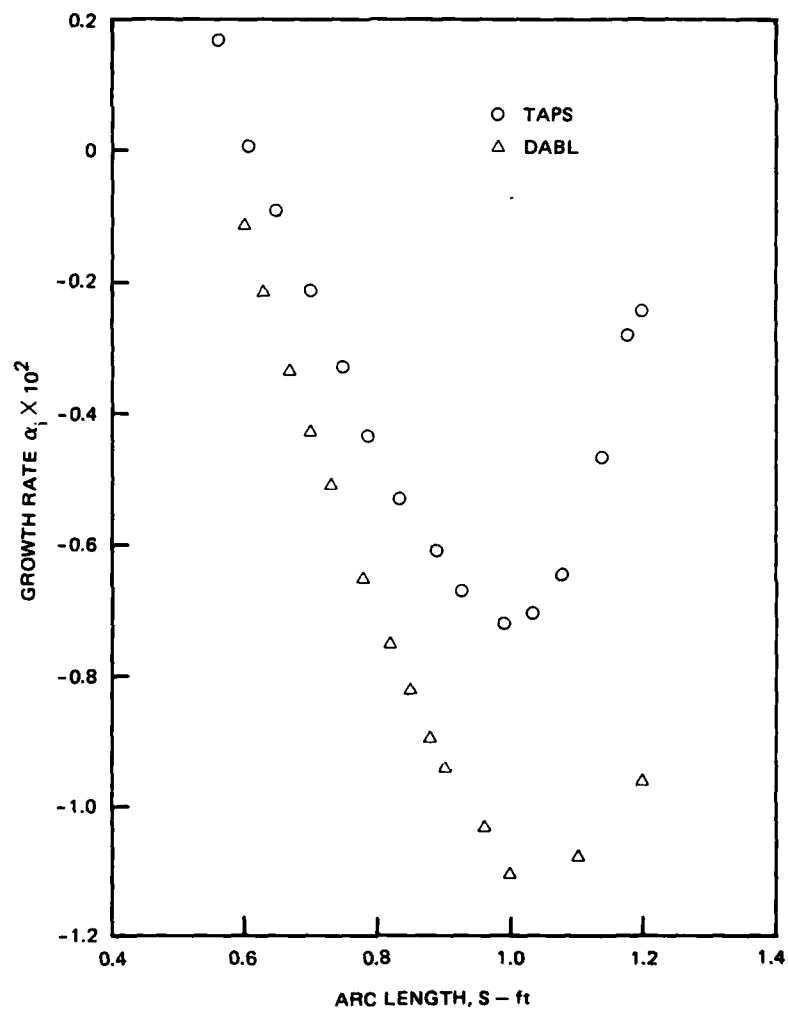


Figure 16. Computed growth rates of a heated 9:1 ellipsoid for $\omega_f = 0.18 \times 10^{-4}$ - $R_L = 4\,490\,1734 \times 10^6/\text{ft}$.

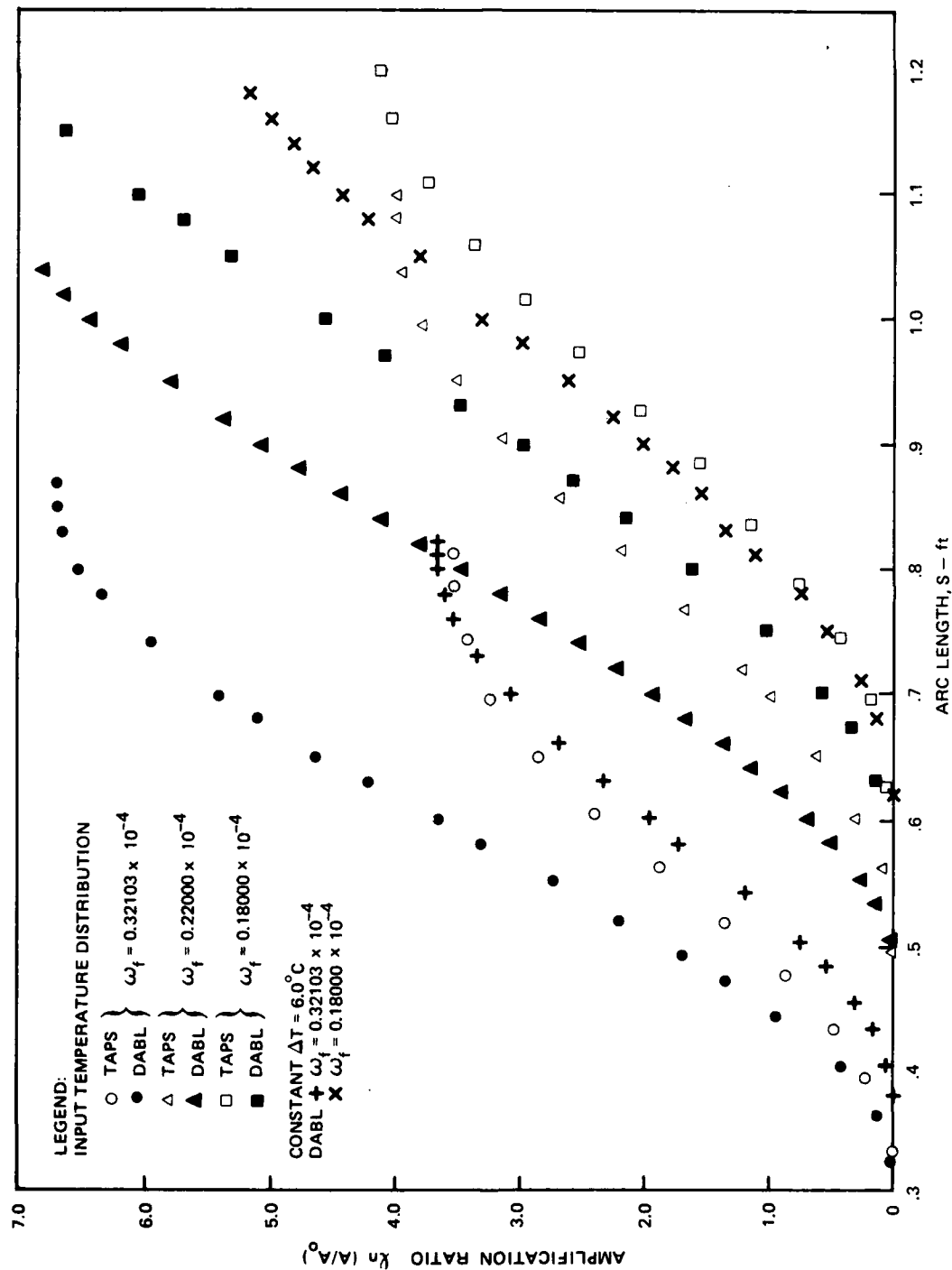


Figure 17. Comparison of the computed amplification ratios for a heated 9:1 ellipsoid - $R_L = 4.4901734 \times 10^6/\text{ft}$.

COMPUTER PROGRAM USAGE

DEFINITION OF THE INPUT VARIABLES

VARIABLE	DESCRIPTION
IBL	<p>If IBL = 0, calculate the boundary layer properties and perform the stability analysis</p> <p>If IBL = 1, calculate the boundary layer properties to separation or the end of the body</p>
IBLTP	<p>If IBLTP = 0, do not read or write boundary layer data to unit 8</p> <p>If IBLTP = 1, write boundary layer data to unit 8</p> <p>If IBLTP = 2, read boundary layer data from Unit 8</p>
IHEAT	<p>If IHEAT = 0, unheated boundary layer</p> <p>If IHEAT = 1, heated boundary layer</p>
IPOT	<p>If IPOT = 0, calculate potential flow</p> <p>If IPOT = 1, calculate potential flow and punch cards</p> <p>If IPOT = 2, input potential flow according to Data Table 4</p>
ISTART	<p>If ISTART = 0, automatic start of the stability analysis</p> <p>If ISTART = 1, the user provides information – Data Table 2 – for starting/restarting the stability calculations</p>
ITWOD	<p>If ITWOD = 0, axisymmetric body</p> <p>If ITWOD = 1, 2-D body's lower surface</p> <p>If ITWOD = 2, 2-D body's upper surface</p>
IFIT	<p>IFIT controls the amount of boundary layer velocity and temperature profile data used in the stability analysis at each station</p> <p>If IFIT = 1, use every point – normal option</p> <p>If IFIT = 2, use every second point, etc.</p>
IKFZ	<p>If IKFZ = 0, stability analysis stops when the disturbances no longer experience amplification</p> <p>If IKFZ = 1, stability analysis proceeds regardless of amplification</p>
IVISC	<p>If IVISC = 1, water boundary layer</p> <p>If IVISC = 2, air boundary layer</p>
NP	<p>Number of body offsets</p> <p>NP ≤ 160 axisymmetric body</p> <p>NP ≤ 101 2-D body</p>
IBEG	<p>If IBEG = 0, stability analysis autostart begins at station 1</p> <p>If IBEG ≠ 0, stability analysis autostart begins at station X(IBEG)</p>

VARIABLE	DESCRIPTION
KF	<p>The number of nondimensional frequencies for which the amplification ratio is computed</p> <p>If ISTART = 0, $3 \leq KF \leq 10$</p> <p>If ISTART = 1, $1 \leq KF \leq 10$</p> $\omega_f)_{i+1} = 0.83 \omega_f)_i$
BEPS	<p>The convergence criteria in the iteration for the stagnation point in the boundary layer code</p> <p>BEPS = 0.0001 is the recommended value</p>
BLDELS	Arc length increment to be used in the boundary layer calculation
DELS	The estimated arc length spacing at which the instability growth rates are to be computed. The program varies DELS as needed.
TOL	<p>The accuracy to be maintained in the integration of the stability equation</p> <p>TOL = 0.001 is the recommended value</p>
EPS	<p>The convergence criteria for the eigenvalue integration</p> <p>EPS = 0.001 is the recommended value</p>
X	Input abscissa
Y	Input ordinate
OMU	Nondimensional frequency ω_f for which the amplification ratios are to be computed
SO	Arc length starting values for the stability calculations corresponding to OMU
RL	<p>Reynolds number = $U_\infty L / \nu_\infty$</p> <p>Where U_∞ is the free stream velocity (ft/sec);</p> <p>ν_∞ is the kinematic viscosity (ft²/sec); L is a reference length</p>
ANORM	A normalization factor; the X, Y input offsets are divided by ANORM
R1	<p>Displacement thickness Reynolds number at the last completed station; it is input only when restarting the stability calculations – ISTART = 1</p> <p>If ISTART = 0; R1 = 0</p>
U1	<p>Potential flow surface velocity at the last completed station; it is input only when restarting the stability calculations – ISTART = 1</p> <p>If ISTART = 0, U1 = 0</p>
JMAX	<p>The number of points across the boundary layer at which the velocity profiles are computed</p> <p>JMAX \leq 201</p> <p>JMAX = 201 is the recommended value</p>
ETA	<p>The scaled edge of the boundary layer</p> <p>ETA = 6.0 is the normal input</p>
ALFRU	The starting estimate or the value at the last completed station SO for the wave number (α_r^*); it cannot be zero and is usually less than 0.5 for a starting estimate

VARIABLE	DESCRIPTION
ALFIU	The starting estimate or the value at the last completed station SO for the disturbance growth rate (α_1^*); a value of zero will usually suffice as a starting estimate
AMP	The value of the amplification ratio at the last completed station SO or zero for a starting estimate
ITT	A control for the type of temperature distribution If ITT = 0, no heating If ITT = 1, a step function temperature distribution If ITT = 2, a linear temperature distribution If ITT = 3, temperature is given at each input x offset
ITEMP1	The station number corresponding to the offset at which the surface temperature variation is to begin If ITT = 3, ITEMP1 = 0
ITEMP 2	The station number corresponding to the offset at which the surface temperature variation is to end If ITT = 3, ITEMP2 = 0
TEMPI	The free stream temperature in degrees Celsius
DTEMP	The difference in temperature ΔT in Celsius between the free stream temperature and the maximum body temperature If ITT = 3, DTEMP = 0
T	The body temperature corresponding to the x input offsets
UB	The potential flow surface velocities
XC	The scaled abscissa corresponding to the maximum 2-D body diameter
YC	The scaled ordinate corresponding to the midpoint of the maximum diameter
ANGO	The angle of attack in radians

METHOD OF INPUTTING DATA TABLES

The input data tables of body coordinates, temperature distribution and potential flow are input as shown below.

Body Coordinates

Card Columns	F Format					
	1 - 10	11 - 20	21 - 30	31 - 40	41 - 50	51 - 60
	X ₁	X ₂	X ₃
	X _{NP}		
	Y ₁	Y ₂	Y ₃
	Y _{NP}		

Temperature Distribution

Card Columns	F Format					
	1 - 10	11 - 20	21 - 30	31 - 40	41 - 50	51 - 60
	T_1	T_2	T_3
	T_{NP}		

Potential Flow Surface Velocities

Card Columns	F Format					
	1 - 10	11 - 20	21 - 30	31 - 40	41 - 50	51 - 60
	UB_1	UB_2	UB_3
	UB_{NP-1}		

PROGRAM INPUT SCHEME

Label Card

Card Columns	Format	Variable
1 - 60	A	TITLE

Flag Card

Card Columns	Format	Variable
1	I	IBL
3	I	IBLTP
5	I	IHEAT
7	I	IPOT
9	I	ISTART
11	I	ITWOD
13	I	IFIT
15	I	IKFZ
17	I	IVISC
19 - 21	I	NP
23 - 25	I	IBEG
27 - 29	I	KF

Constant Card 1

Card Columns	Format	Variable
1 - 20	F	RL
21 - 30	F	ANORM
31 - 40	F	R1
41 - 50	F	U1

Constant Card 2

Card Columns	Format	Variable
1 - 3	I	JMAX
11 - 20	F	ETA
21 - 30	F	BEPS
31 - 40	F	BLDELS
41 - 50	F	DELS
51 - 60	F	TOL
61 - 70	F	EPS

Data Table 1: Body Coordinates $Y = f(x)$

The maximum number of entries this table may contain is:

- a) NP = 160 for an axisymmetric body
- b) NP = 101 for a two-dimensional body

Figure 18 illustrates the method used to input the coordinates for an axisymmetric body while Figure 19 should be used for two-dimensional bodies.

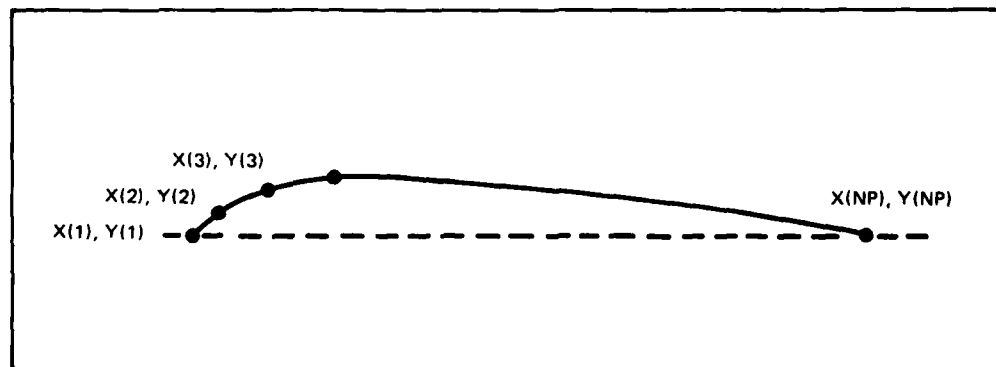


Figure 18. Input direction for the axisymmetric body coordinates.

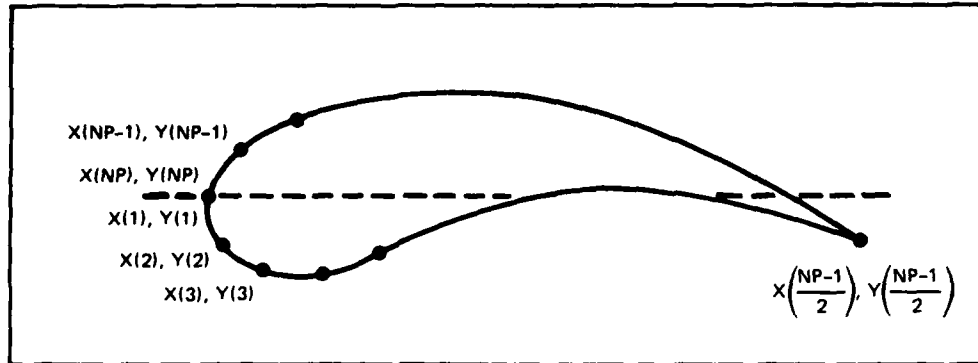


Figure 19. Input direction for the two-dimensional body coordinates.

Data Table 2: Start/Restart Information for the Stability Calculations

If ISTART = 0, do not input this table. The number of entries is $1 \leq KF \leq 10$.

Card Columns	Format	Variable
1 - 10	E	OMU(I)*
11 - 20	F	SO (I)
21 - 30	F	ALFRU (I)
31 - 40	F	ALFIU (I)
41 - 50	F	AMP (I)

*Note: Repeat this card for each value of OMU ($I = 1, KF$).

Constant Card 3

If IHEAT = 0, do not input this card.

Card Columns	Format	Variable
1	I	ITT
3 - 5	I	ITEMP1
7 - 9	I	ITEMP2
11 - 20	F	TEMP1
21 - 30	F	DTEMP

Data Table 3: Body Surface Temperature Distribution $T = f(x)$

If IHEAT = 0 or ITT \neq 3, do not input this table.

The number of entries in this table is NP.

Each input temperature corresponds to each input x offset - Data Table 1.

For two-dimensional bodies, the surface temperature distribution follows the input scheme of Figure 19.

Data Table 4: Potential Flow Surface Velocities $UB = f(x)$

The number of entries in this table is NP-1.

The potential flow velocities are at the midpoints of the input x offsets – Data Table 1.

For two-dimensional bodies, the potential flow velocities follow the input scheme of Figure 19.

Constant Card 4

If IPOT = 2 and ITWOD = 0, do not input this card.

Card Columns	Format	Variable
1 - 10	F	XC
11 - 20	F	YC
21 - 30	F	ANGO

COMPUTER PRINTOUT**INCLUDED ITEMS**

All input quantities are printed out to allow for rapid checking for errors. The following section contains the definitions of those output variables not previously defined. Below is a list of the items included in the program output.

1. Control parameters
2. Input body coordinates
3. Start/Restart variables for the stability calculations (ISTART = 1)
4. Temperature control variables
5. Input temperature distribution (IHEAT = 1, ITT = 3)
6. Normalized body coordinates and temperature distribution (IHEAT = 1)
7. Boundary layer parameters
8. Stability autostart variables (ISTART = 0)
9. Stability calculations (IBL = 0)

PRINTOUT DEFINITIONS**Boundary Layer Parameters**

VARIABLE	DEFINITION
S	The computed arc length values at which the boundary layer calculations are made
UEF	Potential flow surface velocity
DUE	Derivatives of the potential flow surface velocity with respect to arc length
RADIUS	Body radius

VARIABLE	DEFINITION
BETA	The Hartree parameter
GAMMA	A boundary layer scale factor
DELTN	Nondimensional boundary layer thickness times $\sqrt{R_L}$
DI	Nondimensional displacement thickness times $\sqrt{R_L}$
H	The boundary layer shape factor
CT	The wall skin friction coefficient times $\sqrt{R_L}$
CQ	Nondimensional local heat transfer coefficient divided by $\sqrt{R_L}$
VISCR	The ratio of fluid viscosity at the wall to that of the ambient fluid

Note: To obtain the actual value of the nondimensional boundary layer thickness, displacement thickness, skin friction coefficient and heat transfer coefficient, divide DELTN, DI and CT by $\sqrt{R_L}$ and multiply CQ by $\sqrt{R_L}$.

Stability Automatic Start

VARIABLE	DEFINITION
S	The arc length
RC	The critical displacement thickness Reynolds number
RD	The displacement thickness Reynolds number
ALPHAC	The critical value α_c of α
OMEGAC	The critical frequency associated with the critical displacement thickness Reynolds number

Stability Calculations

VARIABLE	DEFINITIONS
S	The arc length
U	The potential flow surface velocity
H	The boundary shape factor
DI	The nondimensional displacement thickness times $\sqrt{R_L}$
CT	The wall skin friction coefficient times $\sqrt{R_L}$
R	The displacement thickness Reynolds number
XI	A boundary layer scale factor
RADIUS	The body radius
OMU	The nondimensional frequency - ω_f
ALFRU	The real part of the complex wave number - α^*

VARIABLE	DEFINITIONS
ALFIU	The relative growth rate of the disturbance – imaginary part of α^*
AMP	The amplification ratio A/A_0
ITER	The number of times the eigenvalue problem is solved
NSTEP	The number of integration steps of the Orr-Sommerfeld integration

Note: The DABL code solves the adjoint Orr-Sommerfeld problem where the complex conjugate of α is the eigenvalue. Therefore the output yields

$$\begin{array}{lcl}
 \text{ALFRIU} \equiv \text{Im}(\alpha^*) < 0 & \text{Damped} & \\
 & = 0 & \text{Neutral} \\
 & > 0 & \text{Amplified}
 \end{array}
 \left. \vphantom{\begin{array}{l} \\ \\ \end{array}} \right\} \text{Disturbance}$$

SUMMARY

Several examples illustrating the use of DABL for heated and unheated, two-dimensional and axisymmetric bodies have been presented. For both a heated and unheated flat plate, DABL's automatic starting mode calculated *nondimensional frequencies* which resulted in neutral stability points falling within the previously defined neutral curves. In general, DABL produces unconservative neutral point estimates for the unheated plate and conservative estimates for the heated plate. However, for the unheated plate, when the Reynolds number and disturbance frequencies are reduced, the results fall closer to the neutral curve. Also, the amplification ratios calculated by DABL, for the unheated plate, compare favorably with published results.

The boundary layer properties, growth rates and amplification ratios computed by DABL for an unheated 9:1 ellipsoid compare favorably with the results of TAPS. However, for the heated 9:1 ellipsoid, DABL consistently calculated larger growth rates and amplification ratios than TAPS even though there is close agreement in the calculated boundary layer properties. From these results it can be concluded that DABL produces conservative results for heated axisymmetric bodies.

The DABL computer code can be considered an effective tool in performing parametric design studies for both heated and unheated bodies. For unheated bodies, DABL can be used for predicting the location of boundary layer transition by the e^N method. With its straight forward input scheme, DABL is easy to use and requires a minimum of user interaction.

REFERENCES

1. C. Basset, Private communication – TAPS computations.
2. J. P. Giesing, Extension of the Douglas Neuman Program to Problems of Lifting, Infinite Cascades, Douglas Aircraft Report LB31653 (1964).
3. R. Jordinson, The Flat Plate Boundary Layer. Part 1. Numerical Integration of the Orr-Sommerfeld Equation, Journal of Fluid Mechanics, Vol. 43, Part 4, pp. 801–811 (1970).
4. J. A. Ross, R. H. Barnes, J. G. Burns and M. A. S. Ross, The Flat Plate Boundary Layer. Part 3. Comparison of Theory with Experiment, Journal of Fluid Mechanics, Vol. 43, Part 4, pp. 819–832 (1970).
5. G. B. Schubauer and H. K. Skramstad, Laminar Boundary Layer Oscillations and Transition on a Flat Plate, NACA Report 909 (1948).
6. A. J. Strazisar, Experimental Study of the Stability of Heated Laminar Boundary Layers in Water, PhD thesis, Case Western Reserve University (1976).
7. C. vonKerczek and N. C. Groves, Disturbance Amplification in Boundary Layers, DTNSRDC Report 78/004 (1978).

APPENDIX A

This appendix contains an abbreviated computer printout of the automatic start – stability analysis of a heated flat plate.

DABL - 9:1 ELLIPSOID - HEATED

CONTROL PARAMETERS

IAL= 0 IRLTP= 0 IHEAT= 1 IPOT= 2
 ISTART= 1 ITWOD= 0 IFIT= 1 IKFZ= 0 IVISC= 1
 IIP= 04 IREG= 0 KFI= 2

PI= 4490173.3750 AMORH= 1.000000

JMAX= 201 ETA= 5.000000 DEFS= .001000 ALDELS= .005000
 DELS= .001000 TOL= .001000 EPS= .001000

INPUT BODY COORDINATES

X	Y
.00000	.00000
.20813-001	.19147-001
.41647-001	.27167-001
.62500-001	.33029-001
.83333-001	.37857-001
.10417+000	.42008-001
.12500+000	.45647-001
.14583+000	.48944-001
.16667+000	.51912-001
.18750+000	.54621-001
.20813+000	.57102-001
.22917+000	.59402-001
.25000+000	.61523-001
.27083+000	.63489-001
.29167+000	.65314-001
.31250+000	.67007-001
.33333+000	.68585-001
.35417+000	.70044-001
.37500+000	.71457-001
.39583+000	.72866-001
.41667+000	.73832-001
.43750+000	.74908-001
.45833+000	.75898-001
.47917+000	.76808-001
.50000+000	.77614-001
.52083+000	.78181-001
.54167+000	.79061-001
.	.
.	.
.	.

THIS PAGE IS BEST QUALITY PRACTICABLE
 FROM COPY

RESTART OF THE STABILITY CALCULATIONS

PI= 1880.000 U1= 1.040

I= 1 04U11= .321000-004 SO= .50000 ALFRU11= .19211 ALFIU= .00700 AMP11= 1.87100

I= 2 04U11= .220000-004 SO= .50000 ALFRU11= .20000 ALFIU= .00000 AMP11= .00000

BODY BOUNDARY LAYER - HEATED

ITT= 3 TEMPI= 10.10000 DTEMP= 7.37000 ITEMP1= 1 ITEMP2= 84

INPUT TEMPERATURE DISTRIBUTION

X	TEMP
.00000	.30040+002
.20813+001	.30040+002
.41647+001	.30000+002
.62500+001	.31000+002
.83333+001	.31400+002
.10417+000	.31740+002
.12500+000	.31860+002
.14583+000	.32000+002
.16667+000	.32400+002
.18750+000	.32700+002
.20813+000	.33140+002
.22917+000	.33250+002
.25000+000	.33500+002
.27083+000	.33700+002
.29167+000	.33850+002
.31250+000	.34070+002
.33333+000	.34250+002
.35417+000	.34330+002
.37500+000	.34450+002
.39583+000	.34400+002
.41667+000	.34700+002
.43750+000	.34830+002
.45813+000	.34700+002
.47917+000	.35050+002
.	.
.	.
.	.

POTENTIAL FLOW SOLUTION AND TEMPERATURE DISTRIBUTION
 $X=X/\Delta HORM$, $Y=Y/\Delta HORM$

X	Y	S	U	T
.00000	.00000	.14216-001	.79461+000	.30040+002
.20833-001	.19349-001	.39559-001	.97418+000	.30040+002
.41667-001	.27167-001	.61506-001	.98902+000	.30270+002
.62500-001	.33029-001	.83019-001	.99927+000	.30750+002
.83333-001	.37857-001	.10433+000	.10055+001	.31200+002
.10417+000	.42000-001	.12553+000	.10096+001	.31570+002
.12500+000	.45667-001	.14665+000	.10124+001	.31800+002
.14583+000	.48944-001	.16772+000	.10145+001	.31930+002
.16667+000	.51912-001	.18875+000	.10161+001	.32200+002
.18750+000	.54621-001	.20974+000	.10173+001	.32550+002
.20833+000	.57109-001	.23071+000	.10184+001	.32930+002
.22917+000	.59402-001	.25166+000	.10192+001	.33205+002
.25000+000	.61523-001	.27259+000	.10199+001	.33375+002
.27083+000	.63489-001	.29351+000	.10206+001	.33600+002
.29167+000	.65314-001	.31442+000	.10211+001	.33775+002
.31250+000	.67009-001	.33532+000	.10215+001	.33960+002
.33333+000	.68585-001	.35621+000	.10219+001	.34160+002
.35417+000	.70048-001	.37709+000	.10222+001	.34290+002
.37500+000	.71407-001	.39796+000	.10225+001	.34390+002
.39583+000	.72666-001	.41883+000	.10228+001	.34525+002
.41667+000	.73837-001	.43970+000	.10230+001	.34650+002
.43750+000	.74908-001	.46055+000	.10232+001	.34745+002

THIS PAGE IS A REPRODUCTION FROM COPY FURNISHED TO BDC

.45833+000	.75898-001	.48141+000	.10234+001	.34865+002
.47917+000	.76806-001	.50226+000	.10235+001	.34975+002
.50000+000	.77634-001	.52311+000	.10237+001	.35100+002
.52083+000	.78385-001	.54395+000	.10238+001	.35200+002
.54167+000	.79061-001	.56480+000	.10239+001	.35300+002
.56250+000	.79664-001	.58564+000	.10239+001	.35400+002
.58333+000	.80196-001	.60648+000	.10240+001	.35475+002
.60417+000	.80658-001	.62732+000	.10241+001	.35575+002
.62500+000	.81051-001	.64815+000	.10241+001	.35700+002
.64583+000	.81376-001	.66899+000	.10241+001	.35785+002
.66667+000	.81635-001	.68982+000	.10241+001	.35860+002
.68750+000	.81827-001	.71066+000	.10241+001	.35925+002
.70833+000	.81954-001	.73149+000	.10241+001	.36000+002
.72917+000	.82015-001	.75232+000	.10241+001	.36085+002
.75000+000	.82010-001	.77316+000	.10241+001	.36160+002
.77083+000	.81941-001	.79399+000	.10240+001	.36235+002
.79167+000	.81805-001	.81482+000	.10239+001	.36310+002
.81250+000	.81604-001	.83566+000	.10239+001	.36385+002
.83333+000	.81337-001	.85649+000	.10239+001	.36450+002
.85417+000	.81002-001	.87733+000	.10236+001	.36490+002
.87500+000	.80600-001	.89817+000	.10235+001	.36550+002
.89583+000	.80129-001	.91901+000	.10234+001	.36650+002
.91667+000	.79587-001	.93985+000	.10232+001	.36725+002
.93750+000	.78975-001	.96069+000	.10230+001	.36775+002
.95833+000	.78289-001	.98154+000	.10227+001	.36850+002
.97917+000	.77527-001	.10024+001	.10224+001	.36930+002
.10000+001	.76687-001	.10232+001	.10221+001	.36980+002
.10208+001	.75770-001	.10441+001	.10218+001	.37065+002
.10417+001	.74767-001			.37165+002

.10625+001	.73681-001	.10650+001	.10213+001	.37225+002
.10833+001	.72503-001	.10858+001	.10208+001	.37300+002
.11042+001	.71231-001	.11067+001	.10202+001	.37410+002
.11250+001	.69859-001	.11276+001	.10196+001	.37470+002
.11458+001	.68381-001	.11484+001	.10188+001	.37470+002
.11667+001	.66790-001	.11693+001	.10178+001	.37470+002
.11875+001	.65077-001	.11902+001	.10167+001	.37470+002
.12083+001	.63234-001	.12111+001	.10153+001	.37470+002
.12292+001	.61249-001	.12321+001	.10137+001	.37470+002
.12500+001	.59106-001	.12530+001	.10119+001	.37470+002
.12708+001	.56788-001	.12740+001	.10105+001	.37470+002
.12917+001	.54272-001	.12949+001	.10170+001	.37470+002
.12959+001	.53375-001	.13076+001	.98470+000	.37470+002
.13126+001	.51017-001	.13182+001	.97726+000	.37470+002
.13292+001	.48458-001	.13350+001	.97141+000	.37470+002
.13459+001	.46300-001	.13514+001	.95796+000	.37470+002
.13626+001	.43942-001	.13687+001	.93382+000	.37470+002
.13793+001	.41467-001	.13855+001	.90911+000	.37470+002
.14167+001	.41467-001	.14126+001	.92730+000	.37470+002
.14683+001	.41467-001	.14522+001	.97101+000	.37470+002
.15000+001	.41667-001	.14938+001	.98399+000	.37470+002
.15417+001	.41667-001	.15355+001	.99044+000	.37470+002
.15833+001	.41667-001	.15772+001	.99478+000	.37470+002
.16250+001	.41667-001	.16188+001	.99797+000	.37470+002
.16667+001	.41667-001	.16605+001	.10007+001	.37470+002
.17083+001	.41667-001	.17022+001	.10035+001	.37470+002
.17500+001	.41667-001	.17438+001	.10067+001	.37470+002
.17917+001	.41667-001	.17855+001	.10110+001	.37470+002
		.18272+001	.10176+001	.37470+002

THIS PAGE IS BEST QUALITY PRACTICABLE
FROM COPY FROM THE 10-100

.18333-001	.41667-001	.18888-001	.10288-001	.37470+002
.18750-001	.41667-001	.19105+001	.10489+001	.37470+002
.19167+001	.41667-001	.19522+001	.10747+001	.37470+002
.19583-001	.41667-001	.19938+001	.11004+001	.37470+002
.20000+001	.41667-001			.37470+002

START BOUNDARY LAYER/STABILITY ANALYSIS

S	UEF	NUF	RADIUS	RETA	GAMMA	DELTA	DI	H	CT	CQ	VISC
.5000-000	.3699+000	.6416+002	.3565-002	.9660+000	.8150+001	.2800-001	.6851+000	.2199+001	.7173+001	.7525-002	.1001+001
.1000-001	.6416+000	.9455+002	.6754-002	.4883+000	.9459+001	.2825+001	.7443+000	.2305+001	.1235+002	.8454-002	.1001+001
.1500-001	.9277+000	.3429+002	.1018-001	.3844+000	.9444+001	.2965+001	.8334+000	.2370+001	.1314+002	.5987-002	.1001+001
.2000-001	.9506+000	.1766+002	.1329-001	.2270+000	.8821+001	.3109+001	.8893+000	.2382+001	.1292+002	.5821-002	.1000+001
.2500-001	.1007+001	.5589+001	.1420-001	.8651-001	.7946+001	.3241+001	.9843+000	.2486+001	.1004+002	.1073-001	.9992+000
.3000-001	.1014+001	.1934+001	.1888-001	.3875-001	.7045+001	.3424+001	.1087+001	.2588+001	.7505+001	.1566-001	.9983+000
.3500-001	.9951+000	.4906+001	.2130-001	.1296+000	.6275+001	.3604+001	.1216+001	.2709+001	.4971+001	.1745-001	.9973+000
.4000-001	.7276+000	.3349+001	.2343-001	.1053+000	.5640+001	.3704+001	.1282+001	.2747+001	.4141+001	.2172-001	.9962+000
.4500-001	.9635+000	.4916+001	.2529-001	.1829-001	.5184+001	.3718+001	.1266+001	.2679+001	.4189+001	.3618-001	.9940+000
.5000-001	.9660+000	.1353+001	.2691-001	.5739-001	.4855+001	.3679+001	.1208+001	.2577+001	.4628+001	.4557-001	.9917+000
.5500-001	.7453+000	.2195+001	.2836-001	.1030+000	.4604+001	.3638+001	.1130+001	.2519+001	.4815+001	.5473-001	.9894+000
.6000-001	.9862+000	.2004+001	.2970-001	.1036+000	.4399+001	.3607+001	.1130+001	.2487+001	.4869+001	.6238-001	.9872+000
.6500-001	.9949+000	.1125+001	.3101-001	.6335-001	.4215+001	.3607+001	.1128+001	.2500+001	.4549+001	.6754-001	.9850+000
.7000-001											
.7500-001											
.8000-001											
.8500-001											
.9000-001											
.9500-001											
.1000-002											
.1050-000	.1023+001	.1221-001	.7246-001	.5255-002	.1525+001	.3660+001	.1173+001	.2548+001	.1448+001	.1169+000	.9119+000
.1100-000	.1023+001	.1184-001	.7275-001	.5166-002	.1514+001	.3660+001	.1173+001	.2548+001	.1437+001	.1167+000	.9114+000
.1150-000	.1023+001	.1165-001	.7303-001	.5157-002	.1503+001	.3660+001	.1173+001	.2548+001	.1426+001	.1166+000	.9108+000
.1200-000	.1023+001	.1164-001	.7331-001	.5227-002	.1492+001	.3660+001	.1173+001	.2548+001	.1416+001	.1165+000	.9103+000
.1250-000	.1023+001	.1154-001	.7359-001	.5264-002	.1482+001	.3660+001	.1173+001	.2548+001	.1405+001	.1161+000	.9098+000
.1300-000	.1023+001	.1130-001	.7386-001	.5217-002	.1472+001	.3660+001	.1173+001	.2548+001	.1396+001	.1159+000	.9092+000
.1350-000	.1023+001	.1085-001	.7413-001	.5081-002	.1462+001	.3660+001	.1173+001	.2547+001	.1385+001	.1157+000	.9087+000
.1400-000	.1023+001	.1023+001	.7439-001	.4853-002	.1452+001	.3659+001	.1172+001	.2547+001	.1375+001	.1155+000	.9082+000
.1450-000	.1023+001	.9408+002	.7464-001	.4621-002	.1442+001	.3659+001	.1172+001	.2547+001	.1365+001	.1149+000	.9078+000
.1500-000	.1023+001	.9147+002	.7489-001	.4459+002	.1432+001	.3659+001	.1172+001	.2547+001	.1356+001	.1146+000	.9074+000
.1550-000	.1023+001	.8845+002	.7514-001	.4370+002	.1423+001	.3659+001	.1172+001	.2547+001	.1346+001	.1142+000	.9069+000
.1600-000	.1023+001	.8702+002	.7538-001	.4356+002	.1413+001	.3659+001	.1172+001	.2547+001	.1337+001	.1139+000	.9065+000
.1650-000	.1023+001	.8632+002	.7561-001	.4378-002	.1404+001	.3659+001	.1172+001	.2547+001	.1328+001	.1139+000	.9060+000
.1700-000	.1023+001	.8509+002	.7584-001	.4372+002	.1395+001	.3659+001	.1172+001	.2547+001	.1319+001	.1138+000	.9055+000
.1750-000	.1023+001	.8312+002	.7607-001	.4336+002	.1384+001	.3659+001	.1172+001	.2547+001	.1310+001	.1137+000	.9050+000
.1800-000	.1023+001	.8099+002	.7629-001	.4269+002	.1377+001	.3659+001	.1172+001	.2547+001	.1301+001	.1134+000	.9045+000
.1850-000	.1023+001	.7824+002	.7651-001	.4176+002	.1369+001	.3659+001	.1172+001	.2547+001	.1293+001	.1133+000	.9040+000
.1900-000	.1023+001	.7542+002	.7672-001	.4077+002	.1360+001	.3659+001	.1172+001	.2547+001	.1284+001	.1131+000	.9035+000
.1950-000	.1023+001	.7255+002	.7693-001	.3971+002	.1352+001	.3659+001	.1171+001	.2547+001	.1275+001	.1129+000	.9029+000
.2000-000	.1024+001	.6983+002	.7713-001	.3859+002	.1343+001	.3659+001	.1171+001	.2546+001	.1267+001	.1127+000	.9024+000
.2050-000	.1024+001	.6671+002	.7733-001	.3743+002	.1335+001	.3659+001	.1171+001	.2544+001	.1259+001	.1125+000	.9019+000

S= .50000+000 U= .10235+001 H= .25464+001 DI= .11655+001 CT= .14043+001 R= .18818+004 XI= .17269+002 RADIUS= .77130+001

OHU	ALFRU	ALFIU	AMP	ITER	NSTEP
.32100+004	.19222+000	.70543+002	.18881+001	3	67
.22000+004	.14083+000	.12010+002	.14645+002	8	50

S= .50100+000 U= .10735+001 H= .25464+001 DI= .11655+001 CT= .14026+001 R= .18841+004 XI= .17330+002 RADIUS= .77170+001

OHU	ALFRU	ALFIU	AMP	ITER	NSTEP
.32100+004	.17244+000	.70777+002	.19054+001	3	67
.22000+004	.14098+000	.12490+002	.14564+002	3	50

S= .50200+000 U= .10735+001 H= .25464+001 DI= .11655+001 CT= .14010+001 R= .18864+004 XI= .17391+002 RADIUS= .77210+001

OHU	ALFRU	ALFIU	AMP	ITER	NSTEP
.32100+004	.19266+000	.71011+002	.19227+001	1	63
.22000+004	.14114+000	.12970+002	.17556+002	1	50

S= .50300+000 U= .10735+001 H= .25463+001 DI= .11655+001 CT= .13992+001 R= .18897+004 XI= .17452+002 RADIUS= .77249+001

OHU	ALFRU	ALFIU	AMP	ITER	NSTEP
.32100+004	.19289+000	.71245+002	.19400+001	1	63
.22000+004	.14130+000	.13450+002	.10776+001	1	50

S= .50400+000 U= .10235+001 H= .25463+001 DI= .11654+001 CT= .13975+001 R= .18910+004 XI= .17513+002 RADIUS= .77289+001

OHU	ALFRU	ALFIU	AMP	ITER	NSTEP
.32100+004	.19311+000	.71479+002	.19573+001	1	63
.22000+004	.14144+000	.13930+002	.14105+001	1	50

S	UFF	DUE	RADIUS	BETA	GAMMA	DELTA	DI	H	CT	CQ	VISCR
.500+000	.1024+001	.6671+002	.7733+001	.3743+002	.1335+001	.3659+001	.1171+001	.2546+001	.1259+001	.1140+000	.9019+000
.510+000	.1024+001	.4900+002	.7752+001	.3635+002	.1327+001	.3658+001	.1171+001	.2546+001	.1251+001	.1136+000	.9014+000
.5150+000	.1024+001	.4155+002	.7771+001	.3538+002	.1319+001	.3658+001	.1171+001	.2546+001	.1243+001	.1133+000	.9010+000
.5200+000	.1024+001	.5934+002	.7790+001	.3453+002	.1311+001	.3658+001	.1171+001	.2546+001	.1235+001	.1131+000	.9006+000
.5250+000	.1024+001	.5235+002	.7808+001	.3378+002	.1303+001	.3658+001	.1171+001	.2546+001	.1227+001	.1128+000	.9001+000
.5300+000	.1024+001	.5517+002	.7825+001	.3288+002	.1295+001	.3658+001	.1171+001	.2546+001	.1219+001	.1126+000	.8997+000
.5350+000	.1024+001	.5270+002	.7843+001	.3178+002	.1288+001	.3658+001	.1171+001	.2546+001	.1212+001	.1125+000	.8993+000
.5400+000	.1024+001	.4994+002	.7859+001	.3048+002	.1280+001	.3658+001	.1171+001	.2546+001	.1204+001	.1123+000	.8988+000
.5450+000	.1024+001	.4691+002	.7876+001	.2894+002	.1273+001	.3658+001	.1171+001	.2546+001	.1197+001	.1121+000	.8984+000
.5500+000	.1024+001	.4431+002	.7892+001	.2768+002	.1265+001	.3658+001	.1171+001	.2546+001	.1189+001	.1120+000	.8980+000
.5550+000	.1024+001	.4245+002	.7907+001	.2682+002	.1258+001	.3658+001	.1170+001	.2546+001	.1182+001	.1119+000	.8975+000
.5600+000	.1024+001	.4134+002	.7922+001	.2643+002	.1251+001	.3658+001	.1170+001	.2546+001	.1175+001	.1117+000	.8971+000
.5650+000	.1024+001	.4098+002	.7937+001	.2650+002	.1244+001	.3658+001	.1170+001	.2546+001	.1168+001	.1116+000	.8967+000
.5700+000	.1024+001	.4084+002	.7951+001	.2671+002	.1237+001	.3657+001	.1170+001	.2546+001	.1161+001	.1107+000	.8963+000
.5750+000	.1024+001	.4049+002	.7965+001	.2678+002	.1230+001	.3657+001	.1170+001	.2546+001	.1154+001	.1103+000	.8960+000
.5800+000	.1024+001	.3991+002	.7979+001	.2670+002	.1223+001	.3657+001	.1170+001	.2546+001	.1147+001	.1098+000	.8957+000
.5850+000	.1024+001	.3911+002	.7991+001	.2646+002	.1216+001	.3657+001	.1170+001	.2546+001	.1141+001	.1095+000	.8954+000
.5900+000	.1024+001	.3803+002	.8004+001	.2602+002	.1209+001	.3657+001	.1170+001	.2546+001	.1134+001	.1092+000	.8949+000
.5950+000	.1024+001	.3660+002	.8016+001	.2632+002	.1202+001	.3657+001	.1170+001	.2546+001	.1127+001	.1098+000	.8945+000
.6000+000	.1024+001	.3481+002	.8028+001	.2634+002	.1196+001	.3657+001	.1170+001	.2546+001	.1121+001	.1096+000	.8941+000
.6050+000	.1024+001	.3245+002	.8039+001	.2639+002	.1189+001	.3657+001	.1170+001	.2546+001	.1114+001	.1098+000	.8936+000

APPENDIX B

This appendix contains an abbreviated computer printout of the restart mode for the stability analysis of the heated 9:1 ellipsoid.

DABL - FLAT PLATE UPPER SURFACE - HEATED

CONTROL PARAMETERS

IRL= 0 IRLTP= 0 IHEAT= 1 IPOT= 0
 ISTART= 0 ITWOD= 2 IFIT= 1 IKFZ= 1 IVISC= 1
 NP= 25 INEG= 0 KF= 5

RL= 5000000.0000 ANORM= 12.000000

JMAX= 201 ETA= 6.000000 DEPS= .001000 RLOELS= .002000
 OFLS= .001000 TOL= .001000 EPS= .001000

INPUT BODY COORDINATES

X	Y
.00000	.00000
.20810-001	-.65100-003
.41670-001	-.13020-002
.62500-001	-.19530-002
.83330-001	-.26040-002
.10417+000	-.32550-002
.12500+000	-.39100-002
.14583+000	-.45570-002
.16667+000	-.52080-002
.18750+000	-.58600-002
.20833+000	-.65100-002
.22917+000	-.71610-002
.25000+000	-.78125-002
.27080+000	-.84640-002
.29167+000	-.91150-002
.31250+000	-.97660-002
.33333+000	-.10417-001
.35000+000	-.10417-001
.40000+000	-.10417-001
.50000+000	-.10417-001
.75000+000	-.10417-001
.10000+001	-.10417-001
.15000+001	-.10417-001
.20000+001	-.10417-001
.25000+001	-.10417-001
.30000+001	-.10417-001
.35000+001	-.10417-001

THIS PAGE IS BASED UPON DATA FROM
 FROM COPY 1700000 TO END

.40000+001	-.10417-001
.45000+001	-.10417-001
.50000+001	-.10417-001
.55000+001	-.10417-001
.60000+001	-.10417-001
.65000+001	-.10417-001
.70000+001	-.10417-001
.75000+001	-.10417-001
.80000+001	-.10417-001
.85000+001	-.10417-001
.90000+001	-.10417-001
.95000+001	-.10417-001
.10000+002	-.10417-001
.10500+002	-.10417-001
.11000+002	-.10417-001
.11500+002	-.10417-001
.11750+002	-.10417-001
.11850+002	-.10417-001
.11900+002	-.10417-001
.11950+002	-.10417-001
.12000+002	.00000
.11950+002	.10417-001
.11900+002	.10417-001
.11850+002	.10417-001
.11750+002	.10417-001
.11500+002	.10417-001
.11000+002	.10417-001
.10500+002	.10417-001
.10000+002	.10417-001
.95000+001	.10417-001
.90000+001	.10417-001
.85000+001	.10417-001
.80000+001	.10417-001
.75000+001	.10417-001
.70000+001	.10417-001
.65000+001	.10417-001
.60000+001	.10417-001
.55000+001	.10417-001
.50000+001	.10417-001
.45000+001	.10417-001
.40000+001	.10417-001
.35000+001	.10417-001
.30000+001	.10417-001
.25000+001	.10417-001
.20000+001	.10417-001
.15000+001	.10417-001
.10000+001	.10417-001
.75000+000	.10417-001
.50000+000	.10417-001
.40000+000	.10417-001
.35000+000	.10417-001
.33333+000	.10417-001
.31250+000	.77460-002
.29167+000	.91150-002
.27080+000	.84640-002
.25000+000	.78125-002
.22917+000	.71410-002

.20833+000	.65100-002
.10750+000	.58600-002
.16667+000	.52000-002
.14583+000	.45570-002
.12500+000	.39100-002
.10417+000	.32550-002
.8330-001	.26040-002
.62500-001	.19530-002
.41670-001	.13020-002
.20830-001	.65100-003
.00000	.00000

BODY BOUNDARY LAYER - HEATED

IT= 1 TEMP1= 23.89000 DTCHP= 2.78000 ITEMP1= 1 ITEMP2= 95

POTENTIAL FLOW SOLUTION AND TEMPERATURE DISTRIBUTION
 $X=X/ANORM$, $Y=Y/ANGRM$

X	Y	S	U	T
.00000	.00000	.86834-003	.47480+000	.26670+002
.17358-002	.54250-004	.26054-002	.97290+000	.26670+002
.34725-002	.10850-003	.43425-002	.97979+000	.26670+002
.52083-002	.16275-003	.60792-002	.98395+000	.26670+002
.69442-002	.21700-003	.78162-002	.98754+000	.26670+002
.86806-002	.27125-003	.95533-002	.99071+000	.26670+002
.10417-001	.32583-003	.11290-001	.99337+000	.26670+002
.12152-001	.37975-003	.13027-001	.99566+000	.26670+002
.13889-001	.43400-003	.14764-001	.99805+000	.26670+002
.15625-001	.48833-003	.16501-001	.10001+001	.26670+002
.17361-001	.54250-003	.18238-001	.10026+001	.26670+002
.19098-001	.59675-003	.19775-001	.10048+001	.26670+002
.20833-001	.65100-003	.21711-001	.10071+001	.26670+002
.22567-001	.70533-003	.23448-001	.10092+001	.26670+002

THIS PAGE IS BEST COPY AVAILABLE
 FROM 2025 RELEASE BY NSA

.24306-001	.75958-003	.25186-001	.10087-001	.26670+002
.26042-001	.81383-003	.26723-001	.99030-000	.26670+002
.27777-001	.86808-003	.28486-001	.98659-000	.26670+002
.29167-001	.86808-003	.31744-001	.10057-001	.26670+002
.33333-001	.86808-003	.37514-001	.10092-001	.26670+002
.11667-001	.86808-003	.52097-001	.10154-001	.26670+002
.62500-001	.86808-003	.72730-001	.10036-001	.26670+002
.73333-001	.86808-003	.10418-000	.10055-001	.26670+002
.12500+000	.86808-003	.14585+000	.10027-001	.26670+002
.16667+000	.86808-003	.18751+000	.10017-001	.26670+002
.20833+000	.86808-003	.22918+000	.10014-001	.26670+002
.25000+000	.86808-003	.27085+000	.10013-001	.26670+002
.29167+000	.86808-003	.31251+000	.10012+001	.26670+002
.33333+000	.86808-003	.35418+000	.10011-001	.26670+002
.37500+000	.86808-003	.39585+000	.10011+001	.26670+002
.41667+000	.86808-003	.43751+000	.10011+001	.26670+002
.45833+000	.86808-003	.47918+000	.10011+001	.26670+002
.50000+000	.86808-003	.52085+000	.10011+001	.26670+002
.54167+000	.86808-003	.56251+000	.10011+001	.26670+002
.58333+000	.86808-003	.60418+000	.10012+001	.26670+002
.62500+000	.86808-003	.64585+000	.10012+001	.26670+002
.66667+000	.86808-003	.68751+000	.10013+001	.26670+002
.70833+000	.86808-003	.72918+000	.10015+001	.26670+002
.75000+000	.86808-003	.77085+000	.10016+001	.26670+002
.79167+000	.86808-003	.81251+000	.10019+001	.26670+002
.83333+000	.86808-003	.85418+000	.10024+001	.26670+002
.87500+000	.86808-003	.89585+000	.10039+001	.26670+002
.91667+000	.86808-003	.93751+000	.10090+001	.26670+002
.95833+000	.86808-003			.26670+002

THIS PAGE IS BEST QUALITY PRACTICABLE
FROM COPY FURNISHED TO DDC

.77917*000	.84808*003	.74876*000	.10142*001	.26670*002
.78750*000	.84808*003	.78135*000	.10078*001	.26670*002
.79147*000	.84808*003	.78940*000	.10032*001	.26670*002
.79543*000	.84808*003	.79376*000	.10701*001	.26670*002
.10000*001	.00000	.79797*000	.11369*001	.26670*002

START BOUNDARY LAYER/STABILITY ANALYSIS

S	UFF	DUF	RADIUS	BETA	GAMMA	DELTA	DI	H	CT	CQ	VISCR
.4000-002	.9832*000	.1042*002	.1000*001	.2822-008	.6076*005	.3460*001	.1047*001	.2491*001	.6512*005	-.2819*004	.9421*000
.8000-002	.9876*000	.6597*000	.1300*001	.2647-002	.1573*002	.3529*001	.1135*001	.2591*001	.1973*002	-.7903*000	.9421*000
.1000-001	.9916*000	.1739*001	.1000*001	.1396-001	.1116*002	.3576*001	.1137*001	.2540*001	.1078*002	-.5285*000	.9421*000
.1200-001	.9943*000	.1307*001	.1000*001	.1572-001	.9125*001	.3405*001	.1152*001	.2556*001	.8744*001	-.4285*000	.9421*000
.1400-001	.9970*000	.1386*001	.1000*001	.2210-001	.7918*001	.3609*001	.1148*001	.2543*001	.7764*001	-.3746*000	.9421*000
.1600-001	.9992*000	.1303*001	.1000*001	.2587-001	.7096*001	.3613*001	.1148*001	.2542*001	.6967*001	-.3355*000	.9421*000
.1800-001	.1002*001	.1264*001	.1000*001	.3007-001	.6490*001	.3612*001	.1144*001	.2535*001	.6462*001	-.3050*000	.9421*000
.2000-001	.1005*001	.1409*001	.1000*001	.3389-001	.6020*001	.3610*001	.1141*001	.2530*001	.6062*001	-.2864*000	.9421*000
.2200-001	.1007*001	.9174*000	.1000*001	.2803-001	.5641*001	.3610*001	.1140*001	.2530*001	.5683*001	-.2682*000	.9421*000
.2400-001	.1010*001	.1450*001	.1000*001	.6508-001	.5331*001	.3602*001	.1132*001	.2517*001	.5545*001	-.2555*000	.9421*000
.2600-001	.1001*001	.1202*002	.1000*001	.4796*000	.5006*001	.3507*001	.1037*001	.2367*001	.7050*001	-.2638*000	.9421*000
.2800-001	.9858*000	.1825*001	.1000*001	.1728-002	.2704*001	.3499*001	.1038*001	.2405*001	.5560*001	-.2349*000	.9421*000
.3000-001	.9959*000	.4055*001	.1000*001	.3889*000	.4551*001	.3481*001	.1022*001	.2384*001	.6072*001	-.2342*000	.9421*000
.3200-001	.1010*001	.4435*001	.1000*001	.2257*000	.4433*001	.3431*001	.9883*000	.2350*001	.6207*001	-.2297*000	.9421*000
.3400-001	.1014*001	.1764*001	.1000*001	.7969*002	.4287*001	.3463*001	.1025*001	.2429*001	.5029*001	-.2104*000	.9421*000
.3600-001	.1012*001	.1748*001	.1000*001	.1036*000	.4131*001	.3476*001	.1028*001	.2444*001	.4926*001	-.2041*000	.9421*000
.3800-001	.1008*001	.1385*001	.1000*001	.8720*001	.3985*001	.3479*001	.1042*001	.2449*001	.4669*001	-.1958*000	.9421*000
.4000-001	.1007*001	.4696*000	.1000*001	.3154*001	.3858*001	.3493*001	.1055*001	.2469*001	.4342*001	-.1874*000	.9421*000
.4200-001	.1006*001	.2387*000	.1000*001	.1649*001	.3748*001	.3509*001	.1071*001	.2494*001	.4028*001	-.1796*000	.9421*000
.4400-001	.1007*001	.7401*000	.1000*001	.5551*001	.3651*001	.3512*001	.1074*001	.2493*001	.4003*001	-.1762*000	.9421*000
.4600-001	.1009*001	.1035*001	.1000*001	.8141*001	.3565*001	.3510*001	.1072*001	.2485*001	.3975*001	-.1727*000	.9421*000

STABILITY AUTO START SEARCH FOR RC

S=	.00600	RC=	.891.162	RD=	.038
S=	.00800	RC=	.401.878	RD=	159.290
S=	.01000	RC=	.744.042	RD=	225.907
S=	.01200	RC=	.506.080	RD=	280.620
S=	.01400	RC=	.673.228	RD=	323.145
S=	.01600	RC=	.686.923	RD=	361.609
S=	.01800	RC=	.707.456	RD=	395.195
S=	.02000	RC=	.744.325	RD=	425.753
S=	.02200	RC=	.757.713	RD=	455.126
S=	.02400	RC=	.443.556	RD=	479.594
S=	.02600	RC=	.2835.432	RD=	483.505

THIS PAGE IS BEST QUALITY PRACTICABLE
FROM COPY FROM THE TOP

S	UFF	DUF	RADIUS	BETA	GAMMA	DELTA	DI	H	CT	CQ	VISCR
S=	02900	RC=	3709.964	RD=	486.601						
S=	03000	RC=	3378.383	RD=	500.101						
S=	03100	RC=	0954.582	RD=	503.404						
S=	03200	RC=	1741.434	RD=	541.941						
S=	03300	RC=	1047.185	RD=	568.436						
S=	03400	RC=	1575.911	RD=	589.382						
S=	03500	RC=	615.245	RD=	1172.042						
S=	04200	RC=	087.482	RD=	642.906						
S=	04400	RC=	854.674	RD=	652.533						
S=	04600	RC=	755.428	RD=	678.528						

S=	.03400	RC=	747.695	RD=	675.459
S=	.03400	RC=	1170.453	RD=	689.672
S=	.05000	RC=	1212.104	RD=	705.931
S=	.05200	RC=	1167.452	RD=	724.254
S=	.05400	RC=	946.791	RD=	746.379
S=	.05400	RC=	846.312	RD=	768.921
S=	.05600	RC=	773.979	RD=	787.128
RC=	773.979	RD=	787.128	ALPHA=	
DMFGAC=	.07011748	S=	.05900		

$$c = .58000 - 0n \quad u = .10159 + 0n \quad H = .2512^4 + 0n \quad n / s = .10890 + 0n \quad C T = .35621 + 0n \quad R = .78713 + 0n \quad X I = .52248 - 0n \quad R A D I U S = .10000 + 0n$$

S= .62000-001 U= .10155+001 H= .25090+001 D1= .10881+001 CT= .35627+001 R= .79410+003 X1= .53263-001 RADIUS= .10000+001
 OMU
 .11288-003
 .93693-004
 .77765-004
 .64545-004
 .53573-004
 ALFRU
 .24377+000
 .20857+000
 .17912+000
 .15422+000
 .13307+000
 ALFIU
 -.13789-002
 -.35450-002
 -.65035-002
 -.95971-002
 -.12398-001
 AMP
 .00000
 .00000
 .00000
 .00000
 .00000
 ITER
 4
 4
 4
 3
 3
 NSTEP
 47
 42
 40
 36
 32

S= .60700-001 U= .10148+001 H= .25031+001 D1= .10858+001 CT= .35489+001 R= .80195+003 X1= .54481-001 RADIUS= .10000+001
 OMU
 .11288-003
 .93693-004
 .77765-004
 .64545-004
 .53573-004
 ALFRU
 .24530+000
 .20980+000
 .18009+000
 .15503+000
 .13371+000
 ALFIU
 -.16915-002
 -.36444-002
 -.64833-002
 -.94875-002
 -.12259-001
 AMP
 .00000
 .00000
 .00000
 .00000
 .00000
 ITER
 3
 3
 3
 3
 3
 NSTEP
 47
 43
 40
 37
 33

S= .61440-001 U= .10138+001 H= .24964+001 D1= .10827+001 CT= .35596+001 R= .80981+003 X1= .55942-001 RADIUS= .10000+001
 OMU
 .11288-003
 .93693-004
 .77765-004
 .64545-004
 .53573-004
 ALFRU
 .24733+000
 .21142+000
 .18136+000
 .15603+000
 .13452+000
 ALFIU
 -.23344-002
 -.40028-002
 -.66679-002
 -.95704-002
 -.12278-001
 AMP
 .00000
 .00000
 .00000
 .00000
 .00000
 ITER
 3
 3
 3
 3
 3
 NSTEP
 46
 43
 40
 37
 34

S= .63348-001 U= .10121+001 H= .24875+001 D1= .10780+001 CT= .35585+001 R= .81879+003 X1= .57692-001 RADIUS= .10000+001
 OMU
 .11288-003
 .93693-004
 .77765-004
 .64545-004
 .53573-004
 ALFRU
 .24977+000
 .21136+000
 .18289+000
 .15722+000
 .13544+000
 ALFIU
 -.32698-002
 -.45902-002
 -.70449-002
 -.98179-002
 -.12444-001
 AMP
 .00000
 .00000
 .00000
 .00000
 .00000
 ITER
 3
 3
 3
 3
 3
 NSTEP
 46
 43
 39
 36
 34

THIS PAGE IS BEST QUALITY PRACTICABLE
 FROM COPY FURNISHED TO BDC